Supporting Information

Macrocycle Polymeric Networks Based on a Chair-like Calix[4]pyrrole for the Rapid and Efficient Adsorption of Iodine from Water

Zhiye Zheng, [a] Qiuyuan Lin, [a] Linhuang Xie, [a] Xiaolong Chen, [a] Huan Zhou, [a] Kunhua Lin, [a] Dengsong Zhang, [b] Xiaodong Chi, [c] Jonathan L. Sessler, *[d] and Hongyu Wang*[a]

[a] Department of Chemistry, College of Science, and Center for Supramolecular Chemistry & Catalysis, Shanghai University, 99 Shangda Road, Shanghai, 200444, P. R. China

[b] International Joint Laboratory of Catalytic Chemistry, Department of Chemistry, Research Center of Nanoscience and Technology, College of Sciences, Shanghai University, Shanghai 200444, P. R. China

[c] State Key Laboratory of Materials Processing and Die & Mold Technology, School of Materials Science and Engineering, Huazhong University of Science and Technology, Wuhan 430074, P. R. China

[d] Department of Chemistry, The University of Texas at Austin, 105 E. 24th Street A5300, Austin, Texas 78712, United States

* Corresponding authors.

Hongyu Wang

E-mail: wanghy@shu.edu.cn

Jonathan L. Sessler

E-mail: sessler@cm.utexas.edu

Experimental Section

Materials

Unless otherwise stated, all reagents and solvents were obtained from commercial sources and used without further purification. Column chromatography was performed using 200-300 mesh silica gel unless otherwise indicated. Aqueous solutions of iodine were prepared using deionized water.

Nuclear magnetic resonance (NMR) spectra were recorded on a JEOL 400 MHz spectrometer using tetramethylsilane as the internal standard. ^{1}H NMR and ^{13}C NMR chemical shifts are reported in δ units, parts per million (ppm), relative to the chemical shift of the residual solvent. Solid-state ^{13}C NMR spectroscopic measurements were made using a Bruker 600WB AVANCE NEO instrument. UV-Vis spectra were recorded on an Agilent Cary 5000 spectrophotometer. Molecular masses were determined by laser desorption/ionization time-of-flight mass spectrometry (MALDI-TOF MS). Scanning electron microscopy (SEM) images and energy-dispersive spectroscopy (EDS) measurements of the polymers were performed using a JEOL JSM-7500F microscope. Fourier transform infrared (FT-IR) spectra were measured in transmission mode using a Nicolet iS50 spectrometer and KBr pellets at room temperature. Powder X-ray diffraction patterns were recorded on a Rigaku D/Max2500V/PC X-ray powder diffractometer with Cu-Kα radiation (λ = 0.15418 nm). Thermogravimetric analyses (TGA) were carried out on a DSCQ1000 gravimetric thermal analyzer. The surface area and pore size distribution analyses of the polymers were determined using a Quantachrome Autosorb-IQ2 gas adsorption and pore size analyzer, using N_2 adsorption and desorption at 77 K. Samples were degassed at 100 °C under vacuum for 24 h prior to each N_2 adsorption and desorption analysis. X-ray photoelectron spectra (XPS) were recorded using a Thermofisher ESCALAB 250Xi spectrometer. UV-vis/NIR spectra were recorded on a Perkin-Elmer Lambda 750 spectrometer. Electron paramagnetic resonance (EPR) spectroscopy was carried out on a Bruker EMX Plus spectrometer. Raman spectra were recorded on a Renishaw InVia Raman microscope.

Synthesis

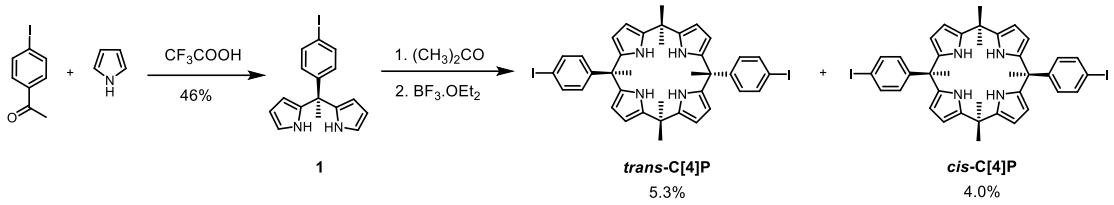

Scheme S1. Synthesis of *trans*-C[4]P. [1]

Synthesis of Compound 1.

A mixture of 4-iodoacetophenone (10.0 g, 40.64 mmol) and 75 mL of pyrrole was stirred at 0 °C. Trifluoroacetic acid (10 mL, 122 mmol) was added over a period of 30 minutes. The mixture was further stirred at room temperature for 3 hours. The reaction was monitored by thin layer chromatography (TLC). Once the reaction was deemed complete, the mixture was poured into 40 mL distilled water and neutralized with 2 M KOH aqueous solution. The aqueous phase was extracted with CH_2Cl_2 (3 × 80 mL). The combined organic phase was dried over anhydrous Na_2SO_4. The solids were filtered off and the volatiles removed under reduced pressure. The resulting residue was purified by column chromatography over silica gel using ethyl acetate/petroleum ether (1:4, v/v) as the eluent to afford a white solid (6.77 g, yield: 46.0%). ^{1}H NMR (400 MHz, $CDCl_3$) δ 7.77 (s, 2H), 7.60-7.55 (d, J = 8.6 Hz, 2H), 6.87-6.82 (d, J = 8.6 Hz, 2H), 6.69-6.65 (m, 2H), 6.18-6.13 (m, J = 3.5 Hz, 2H), 5.96-5.91 (m, 2H), 2.00 (s, 3H). ^{13}C NMR (100 MHz, $CDCl_3$) δ 147.3, 137.2, 136.8, 129.7, 116.9, 108.4, 106.6, 92.4, 44.6, 28.7.

Synthesis of *trans*-C[4]P.

Compound **1** (3.0 g, 8.28 mmol) was dissolved in 225 mL acetone at 0 °C. $BF_3.OEt_2$ (1.1 mL, 9.0 mmol) was then added over a period of 30 minutes. The resulting mixture was stirred at room temperature for 12 hours. The reaction was quenched by adding 200 mL distilled water and the residual acetone was distilled off under reduced pressure. The mixture was neutralized using a 2 M aqueous KOH solution and extracted with CH_2Cl_2 (3 × 100 mL). The combined organic phase was dried over anhydrous Na_2SO_4 and, after filtration, concentrated under reduced pressure to give a mixture of *trans* and *cis* isomers. This crude product was purified by column chromatography over silica gel using ethyl acetate/petroleum ether (5:95, v/v) as the eluent to afford *trans*-C[4]P as a white solid (356 mg, yield: 5.3%). ^{1}H NMR (400 MHz, CD_2Cl_2) δ 7.57-7.54 (d, J = 8.7 Hz, 4H), 7.36-7.23 (s, 4H), 6.84-6.80 (d, J = 8.7 Hz, 4H), 5.89-5.86 (m, 4H), 5.72-5.70 (m, 4H), 1.81 (s, 6H), 1.49 (s, 12H). ^{13}C NMR (100 MHz, CD_2Cl_2) δ

147.0, 139.0, 136.9, 135.8, 129.6, 105.8, 103.2, 91.8, 44.5, 35.2, 29.0, 28.9. MS (MALDI-TOF) calcd for $C_{38}H_{38}I_2N_4$ [M^+] 804.12, found 803.9.

The other isomer, *cis*-C[4]P, was also isolated and set aside. Its spectroscopic data proved in agreement with that reported in the literature.

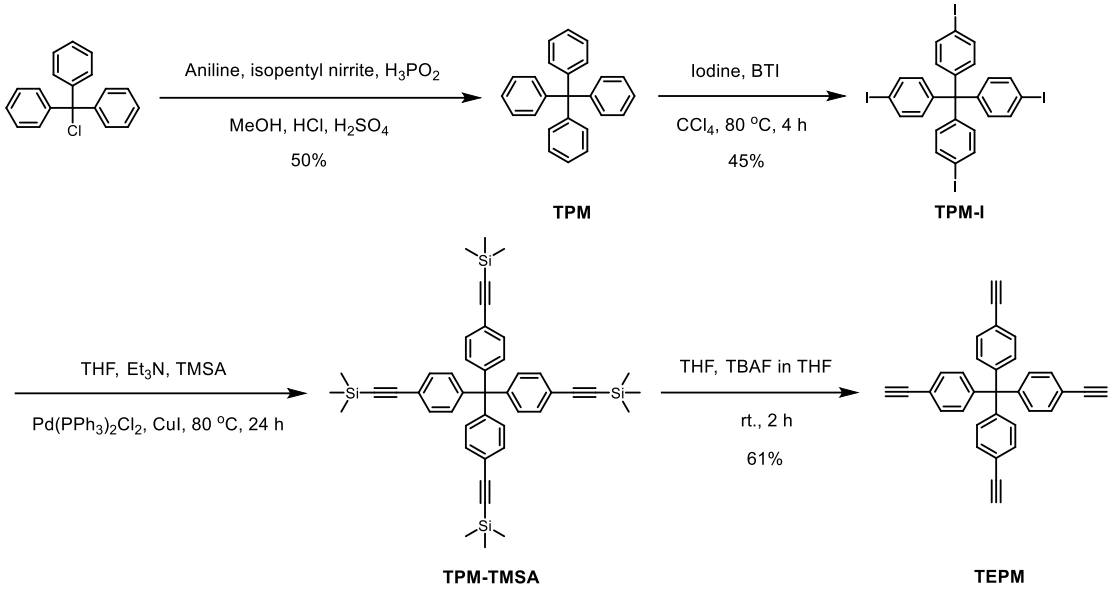

Scheme S2. Synthesis of *tetrakis*-(4-ethynylphenyl)methane (TEPM). [2,3]

Synthesis of TPM.

Aniline (2 mL, 22 mmol) was slowly added into a two-necked round bottom flask containing triphenylmethyl chloride (1.0 g, 3.60 mmol). The flask was then gradually heated to 200 °C. The mixture was stirred at 200 °C for 15 minutes and cooled to 90 °C and held at that temperature for 30 minutes. Subsequently, 8 mL 2 M HCl and 5 mL MeOH were added to the mixture and stirred for 30 minutes. The solid material that resulted was filtered off and washed with 3 mL MeOH. The solid was suspended in 10 mL ethanol and 1 mL concentrated sulfuric acid and cooled to -10°C. Then, 0.8 mL of isopentyl nitrite were added and the reaction stirred for 30 minutes. The mixture was warmed to room temperature and 1.7 mL 50% H_3PO_2 were added. The reaction mixture was then stirred under reflux for 30 minutes. The resulting precipitate was filtered off and washed with 5 mL EtOH to yield a brown solid (0.57 g, yield: 50%). ^{1}H NMR (400 MHz, $CDCl_3$) δ 7.26-7.15 (m, 20H). ^{13}C NMR (100 MHz, $CDCl_3$) δ 146.89, 131.28, 127.56, 125.99, 65.08.

Synthesis of TPM-I.

TPM (1 g, 3.12 mmol), [bis(trifluoroacetoxy)iodo]benzene (4.025 g, 9.36 mmol) and I_2 (2.38 g, 9.38 mmol) were placed in a Schlenk flask under a protective nitrogen atmosphere. Then, 20 mL of CCl_4 were added to the flask using a syringe and the mixture stirred at 60°C for 4 h. The residue was washed with EtOH and the resulting pink solid was suspended in $CHCl_3$ and held

under reflux for 17 h. The resulting precipitate was filtered off and washed with 20 mL $CHCl_3$ to yield a white solid (1.16 g, yield: 45%). ^{1}H NMR (400 MHz, CD_2Cl_2) δ 7.60-7.55 (d, J = 8.8 Hz, 4H), 6.91-6.85 (d, J = 8.7 Hz, 4H).

Synthesis of TEPM.

TPM-I (823 mg, 1.0 mmol), $Pd(PPh_3)_2Cl_2$ (140.6 mg, 0.2 mmol) and cuprous iodide (38.09 mg, 0.2 mmol) were placed in a Schlenk flask under nitrogen atmosphere. Dry THF/triethylamine (25 mL, v/v = 1:1) and trimethylsilylacetylene (2.3 mL, 16 mmol) was added using a syringe. The mixture was then stirred at 80 °C for 24 h. After cooling, the volatiles were removed under reduced pressure. The residue was dissolved in 30 mL of CH_2Cl_2 and washed with brine (3 × 30 mL). The organic phase was concentrated under reduced pressure to give a black solid, TPM-TMSA. This intermediate (TPM-TMSA) was dissolved in toluene/MeCN (18 mL, v/v = 1:1) and 2.5 mL tetrabutylammonium fluoride (1 M in THF, 2.5 mmol) was added. The mixture stirred for 2 h at room temperature before the solvent was removed under reduced pressure. The residue was dissolved in CH_2Cl_2 (30 mL) and washed with brine (3 × 30 mL). The crude product obtained in this way was purified by column chromatography using 100 mesh silica gel as the solid support and ethyl acetate/petroleum ether (1:6, v/v) as the eluent. This afforded TPM-I as a white solid (253.8 mg, yield: 61%). ^{1}H NMR (400 MHz, $CDCl_3$) δ 7.40-7.35 (d, J = 8.6 Hz, 8H), 7.13-7.08 (d, J = 8.8 Hz, 8H), 3.05 (s, 4H). ^{13}C NMR (100 MHz, $CDCl_3$) δ 142.97, 132.68, 130.07, 121.52, 83.25, 77.71, 64.88.

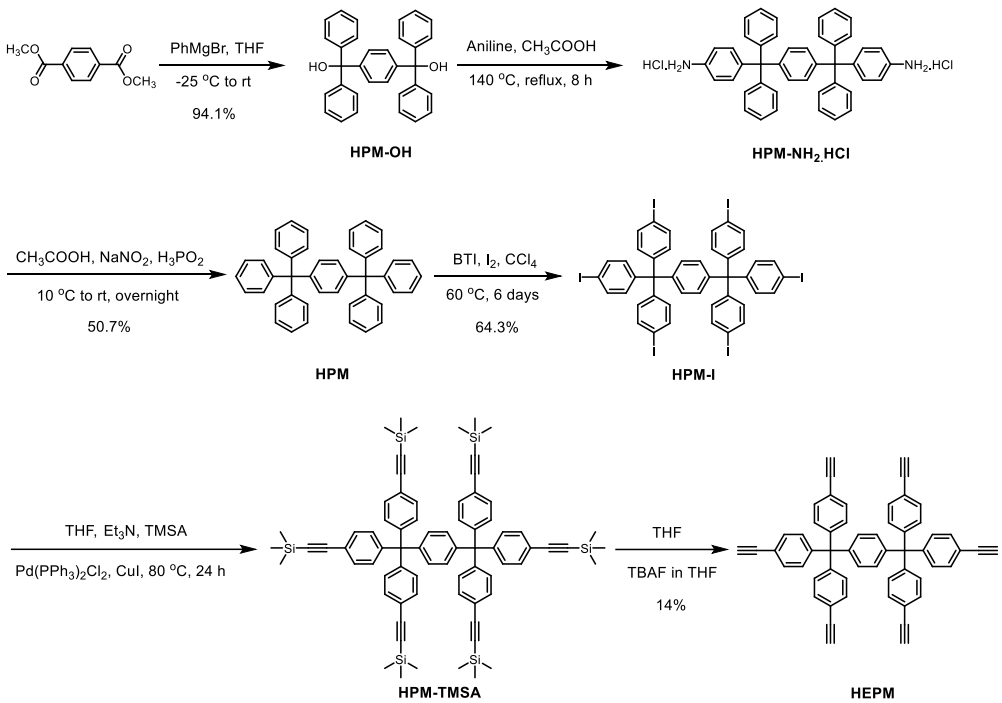

Scheme S3. Synthesis of 1,4-*bis*-[tris(4′-ethynylphenyl)methyl]benzene (HEPM). This precursor was prepared according to a literature reference with minor modification.[4]

Synthesis of HPM-OH.

A two-necked round bottom flask was charged with dimethyl terephthalate (1.2 g, 6.18 mmol) in 40 mL of dry THF under a nitrogen atmosphere. The mixture was cooled to -25 °C, and then 31.2 mL of phenylmagnesium bromide (1.0 M in THF) was added dropwise into the flask. The mixture was further stirred at -25 °C for 20 h. Subsequently, the mixture was heated to room temperature and stirred for additional 4 h. The mixture was poured into a saturated aqueous solution of NH_4Cl (25 mL) and extracted with CH_2Cl_2 (3 × 25 mL). The combined organic layer was dried over anhydrous Na_2SO_4 and, after filtration, concentrated under reduced pressure. The crude product obtained in this way was recrystallized from CH_2Cl_2 and petroleum ether to afford HPM-OH as a white solid (2.57 g, yield: 94.1%). ^{1}H NMR (400 MHz, $CDCl_3$) δ 7.33-7.23 (m, 20H), 7.21 (s, 4H), 2.80 (s, 2H). ^{13}C NMR (100 MHz, $CDCl_3$) δ 146.8, 145.3, 128.0, 127.9, 127.6, 127.4, 81.9.

Synthesis of HPM-NH_2•HCl.

To a round bottom flask was added HPM-OH (1.86 g, 4.2 mmol), aniline (3.64 mL, 39.9 mmol), 2.5 mL concentrated hydrochloric acid and 30 mL of acetic acid. The mixture was stirred at 140 °C for 8 h. Then, the mixture was cooled to room temperature. The resulting precipitate was filtered and washed with 100 mL acetic acid and 100 mL *tert*-butyl methyl ether to yield a white solid. The product was used directly in the next step without further purification or characterization.

Synthesis of HPM.

A mixture of HPM-NH_2•HCl (2.5 g, 3.76 mmol) and sodium nitrite (0.88 g, 12.68 mmol) was dissolved in 225 mL acetic acid and 25 mL phosphinic acid at 10 °C before the mixture was allowed to stir at room temperature overnight. Then, 37.5 mL of distilled water was added to the reaction mixture. The precipitate was filtered and washed with water and MeOH. The residue was purified by column chromatography over silica gel using CH_2Cl_2 as the eluent to afford a white solid (1.21 g, yield: 50.7%). ^{1}H NMR (400 MHz, $CDCl_3$) δ 7.24-7.14 (m, 30H), 7.05 (s, 4H). ^{13}C NMR (100 MHz, $CDCl_3$) δ 146.8, 144.3, 131.3, 130.3, 127.4, 126.0, 64.6.

Synthesis of HPM-I.

A Schlenk flask was charged with HPM (100 mg, 0.18 mmol), [bis(trifluoroacetoxy)iodo]benzene (BTI, 609 mg, 1.416 mmol) and I_2 (269.5 mg, 1.062 mmol) under a nitrogen atmosphere. 10 mL of CCl_4 was then added to the flask using a syringe and the mixture was stirred at 60 °C for 6 days. The volatiles were removed under reduced pressure and the residue suspended in acetone (10 mL) at room temperature for 2 h. At this juncture, the solid was filtered off and washed with acetone to afford HPM as a white solid (150 mg, yield:

64.3%). It was used directly in the next step without further purification. ^{1}H NMR (400 MHz, $CDCl_3$) δ 7.61-7.51 (d, J = 8.7 Hz, 12H), 6.98 (s, 4H), 6.87-6.80 (d, J = 8.7 Hz, 12H). ^{13}C NMR (100 MHz, $CDCl_3$) δ 145.3, 143.5, 137.0, 132.9, 130.3, 92.4, 63.9.

Synthesis of HEPM.

HPM-I (800 mg, 0.607 mmol), $Pd(PPh_3)_2Cl_2$ (85 mg, 0.121 mmol) and cuprous iodide (23 mg, 0.121 mmol) were placed in a Schlenk flask under a nitrogen atmosphere. A mixture of THF/triethylamine (30 mL, v/v = 1:1) and trimethylsilylacetylene (2.1 mL, 14.57 mmol) was added using a syringe and the reaction stirred at 80 °C for 24 h. Then, the volatiles were removed under reduced pressure. The resulting residue was dissolved in 30 mL CH_2Cl_2 and washed with brine (3 × 30 mL). The organic phase was concentrated under reduced pressure to give a black solid. This crude HPM-TMSA product was dissolved in THF (50 mL) and 4 mL tetrabutylammonium fluoride (1 M in THF, 4.0 mmol) were added. The mixture was stirred for 2 h at room temperature before the volatiles were removed under reduced pressure. The resulting residue was dissolved in CH_2Cl_2 (30 mL) and washed with brine (3×30 mL). The crude product obtained in this way was purified by column chromatography over 100 mesh silica gel using ethyl acetate/petroleum ether (1:6, v/v) as the eluent. This gave HEPM as a white solid (60 mg, yield: 14.0%). ^{1}H NMR (400 MHz, $CDCl_3$) δ 7.40-7.34 (d, J = 8.5 Hz, 12H), 7.11-7.06 (d, J = 8.5 Hz, 12H), 7.01 (s, 4H), 3.05 (s, 6H). ^{13}C NMR (100 MHz, $CDCl_3$) δ 146.5, 143.6, 131.6, 130.9, 129.4, 119.3, 82.8, 77.6, 64.5.

Synthesis of C[4]P-TEPM.

Monomer TEPM (50 mg, 0.12 mmol) and *trans*-C[4]P (193 mg, 0.24 mmol), tetrakis-(triphenylphosphine)palladium (29 mg, 0.0252 mmol) and cuprous iodide (8.9 mg, 0.0468 mmol) were placed in a Schlenk flask under a nitrogen atmosphere. A solution of toluene/triethylamine (16 mL, v/v = 1:1) was then added using a syringe. The flask was then degassed by three freeze-pump-thaw cycles. The resulting reaction mixture was vigorously stirred at 90 °C for three days. After allowing to cool to room temperature, the resulting precipitate was filtered and washed successively with excess dichloromethane, 1 mol L^{-1} aqueous HCl, tetrahydrofuran, and acetone. The solid obtained was collected and further purified by Soxhlet extraction with dichloromethane for 24 h to remove unreacted monomers and metal catalyst residues. The final product was dried in vacuum at 80 °C for 24 h to give C[4]P-TEPM as a yellow powder (181 mg, yield: 99.7%).

Synthesis of C[4]P-HEPM.

Using a procedure similar to that used for the preparation of C[4]P-TEPM, C[4]P-HEPM was obtained as a yellow solid in a yield of 99.9% starting from the monomers HEPM (70.69 mg, 0.1 mmol) and *trans*-C[4]P (241.2 mg, 0.3 mmol).

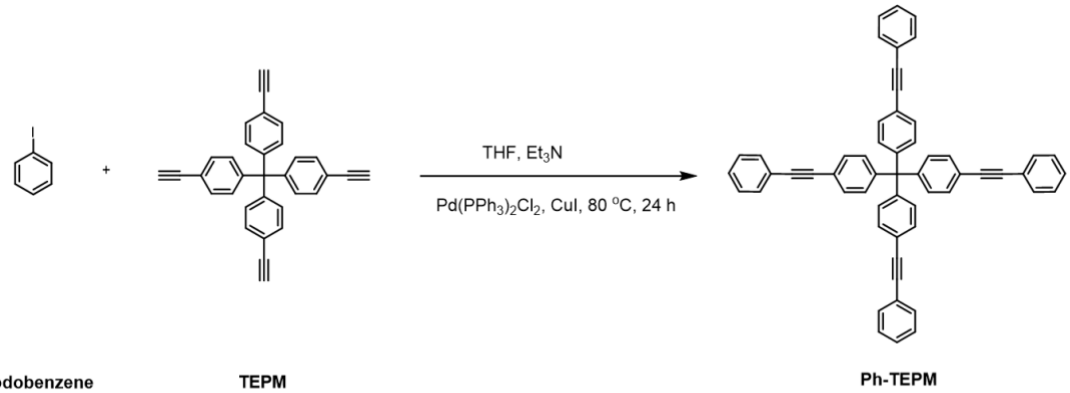

Scheme S4. Synthesis of tetrakis(4-(phenylethynyl)phenyl)methane (**Ph-TEPM**).

Synthesis of Ph-TEPM.

To a Schlenk flask was added **TEPM** (200 mg, 0.48 mmol), iodobenzene (391.84 mg, 1.92 mmol), $Pd(PPh_3)_2Cl_2$ (33.7 mg, 0.048 mmol) and cuprous iodide (9.14 mg, 0.048 mmol) under a nitrogen atmosphere. A mixture of THF/triethylamine (10 mL, v/v = 1:1) was added using a syringe and the reaction stirred at 80 °C for 24 h. Then, the volatiles were removed under reduced pressure. The crude product was purified by column chromatography using 200-300 mesh silica gel as the solid support and dichloromethane/petroleum ether (1:2, v/v) as the eluent to afford white powder (150 mg, yield: 43.3%). ^{1}H NMR (400 MHz, $CDCl_3$) δ 7.54-7.49 (m, 8H), 7.46 (d, J = 8.5 Hz, 8H), 7.36-7.31 (dd, J = 5.1, 2.0 Hz, 12H), 7.21 (d, J = 8.6 Hz, 8H). ^{13}C NMR (100 MHz, $CDCl_3$) δ 146.0, 131.7, 131.1, 131.0, 128.46, 128.44, 123.2, 121.4, 89.8, 89.0, 64.4.

NMR and MS data for compounds prepared in this study

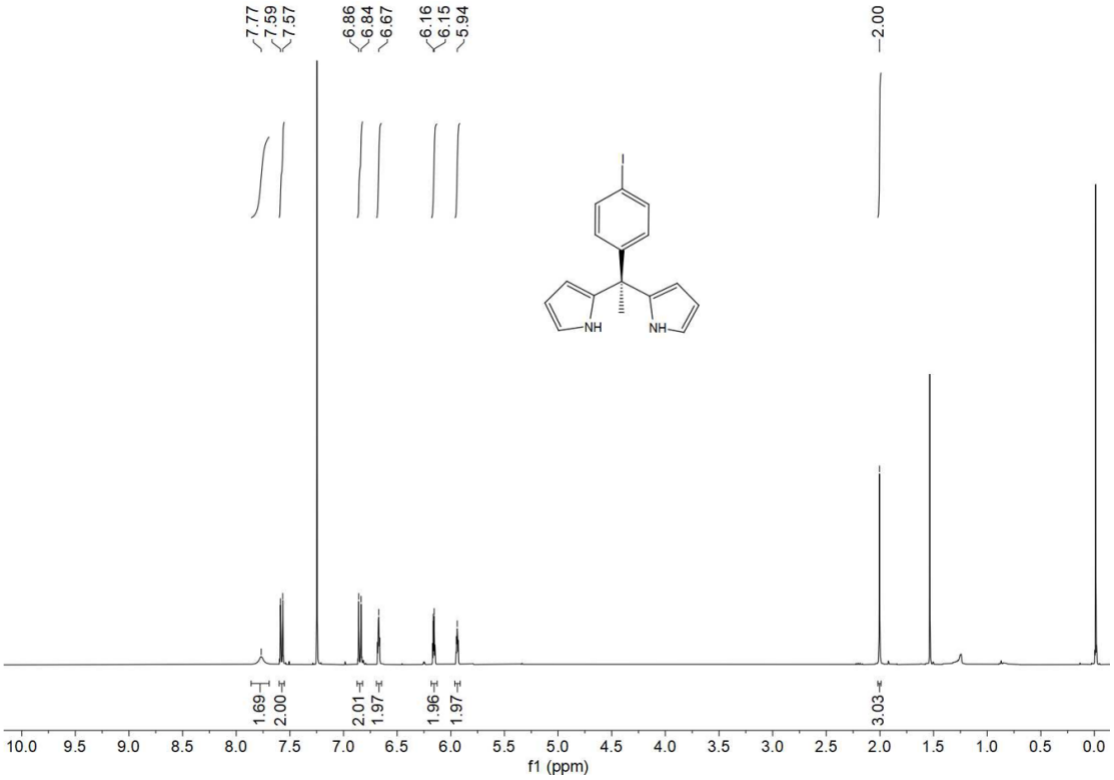

Fig. S1 ^{1}H NMR spectrum of compound **1** in $CDCl_3$.

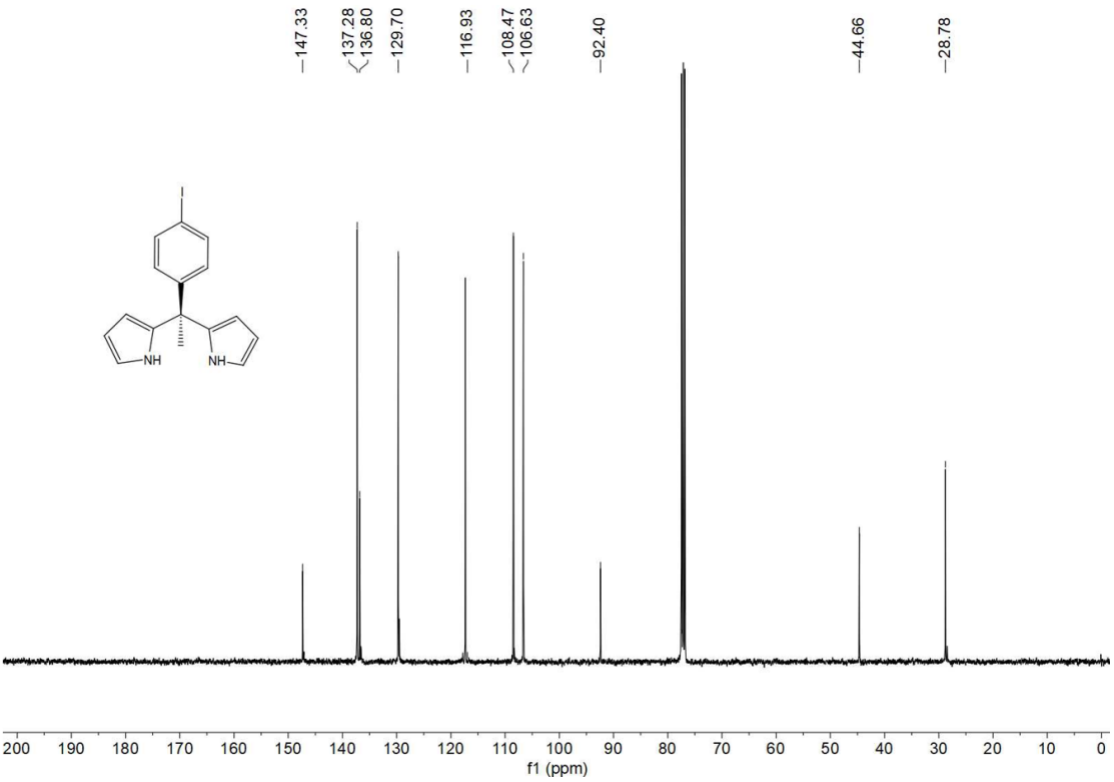

Fig. S2 ^{13}C NMR spectrum of compound **1** in $CDCl_3$.

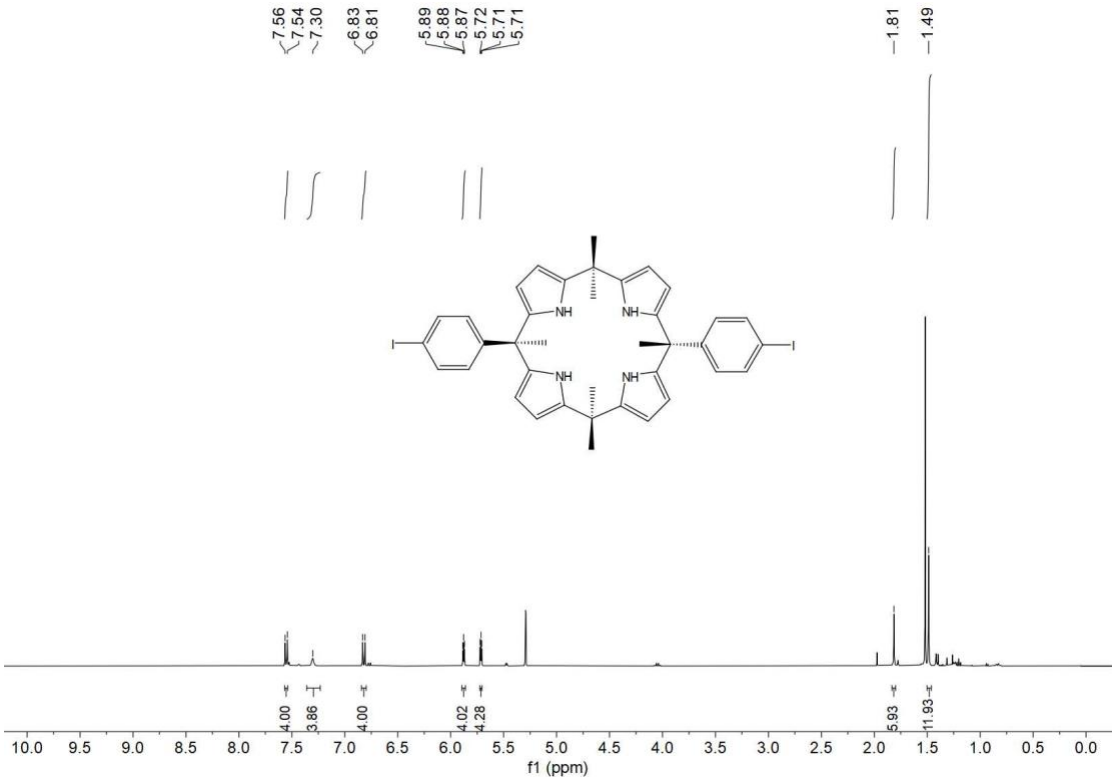

Fig. S3 ^{1}H NMR spectrum of *trans*-C[4]P in CD_2Cl_2.

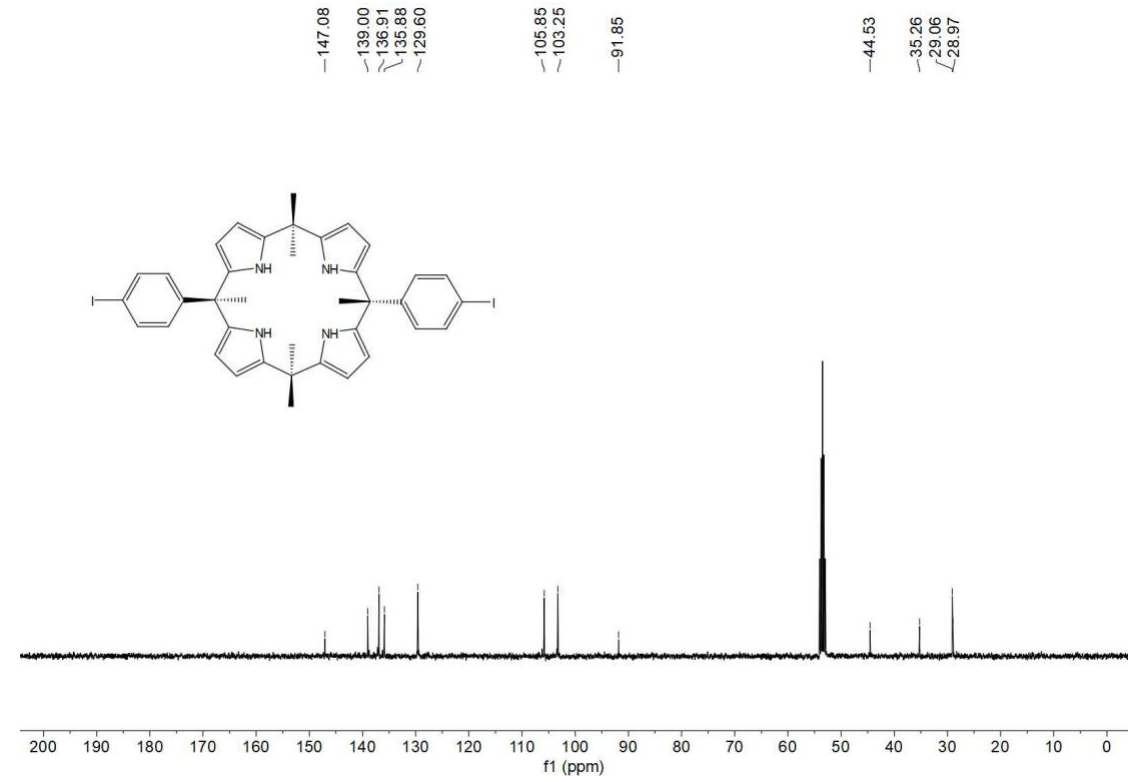

Fig. S4 ^{13}C NMR spectrum of *trans*-C[4]P in CD_2Cl_2.

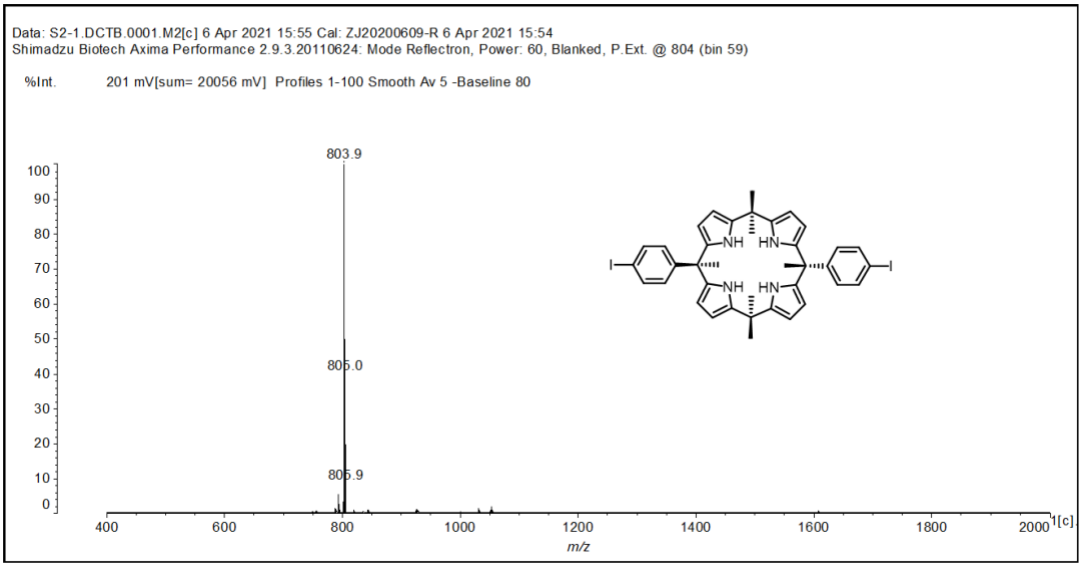

Fig. S5 MALDI-TOF MS spectrum of *trans*-C[4]P.

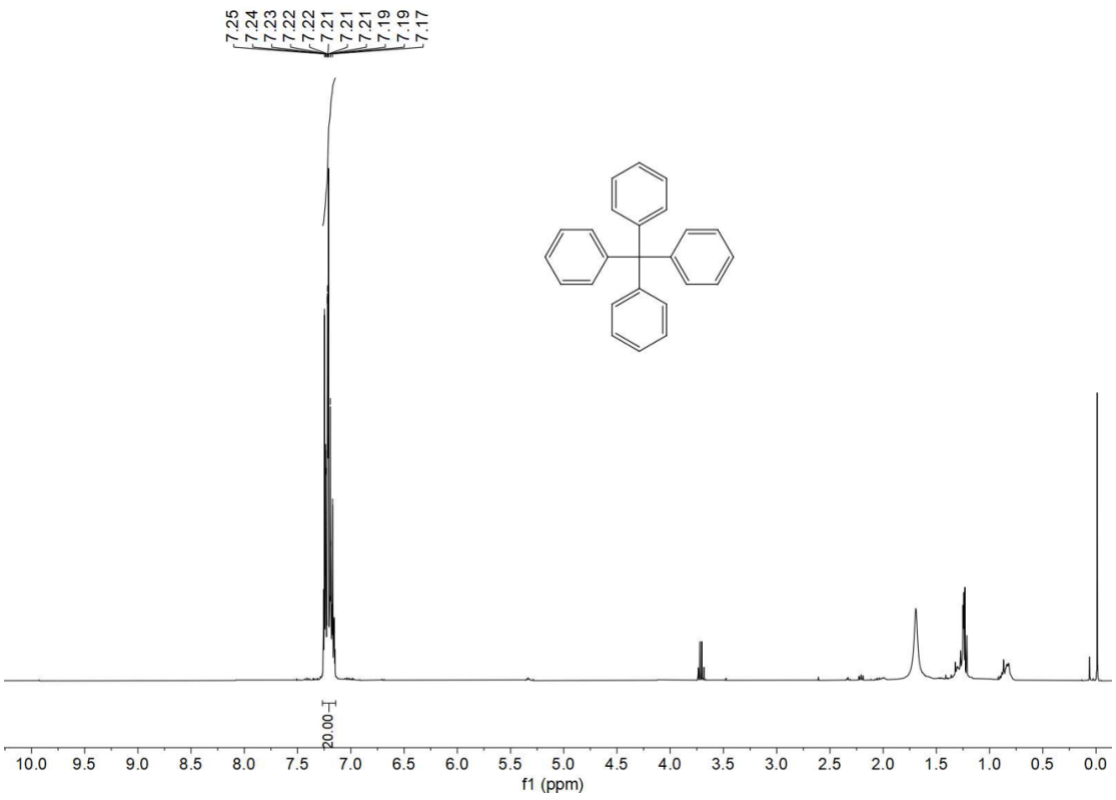

Fig. S6 ^{1}H NMR spectrum of TPM in $CDCl_3$.

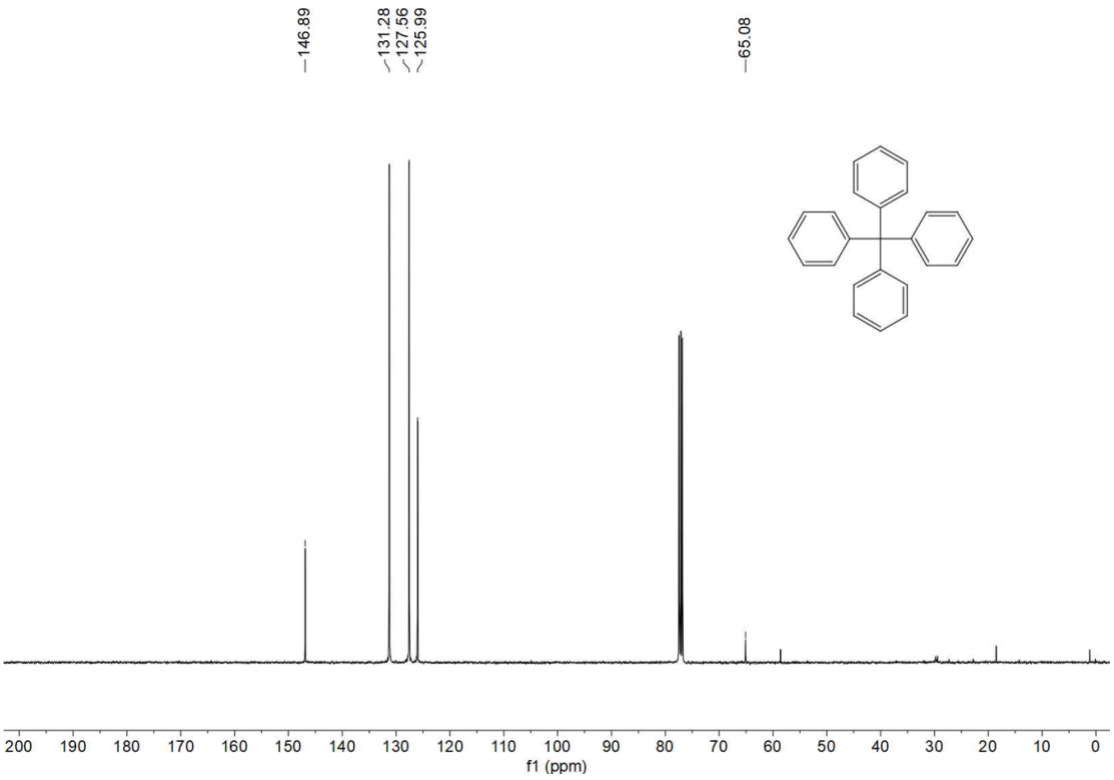

Fig. S7 ^{13}C NMR spectrum of TPM in $CDCl_3$.

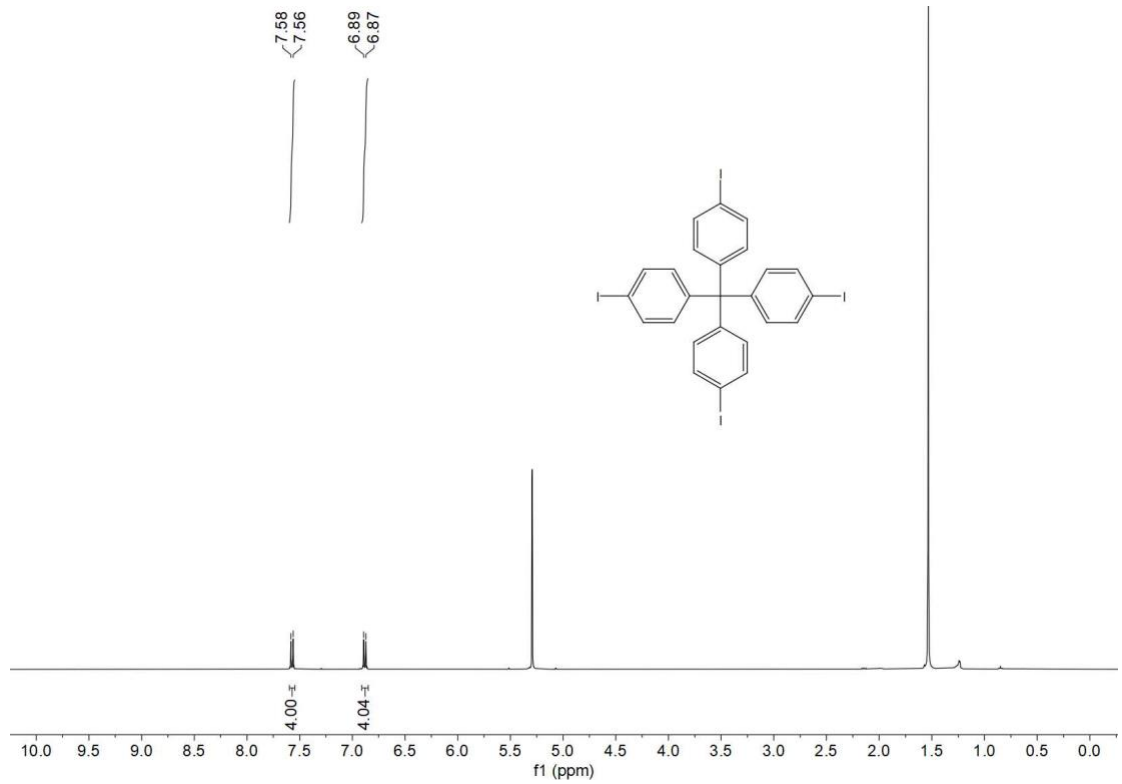

Fig. S8 ^{1}H NMR spectrum of TPM-I in CD_2Cl_2.

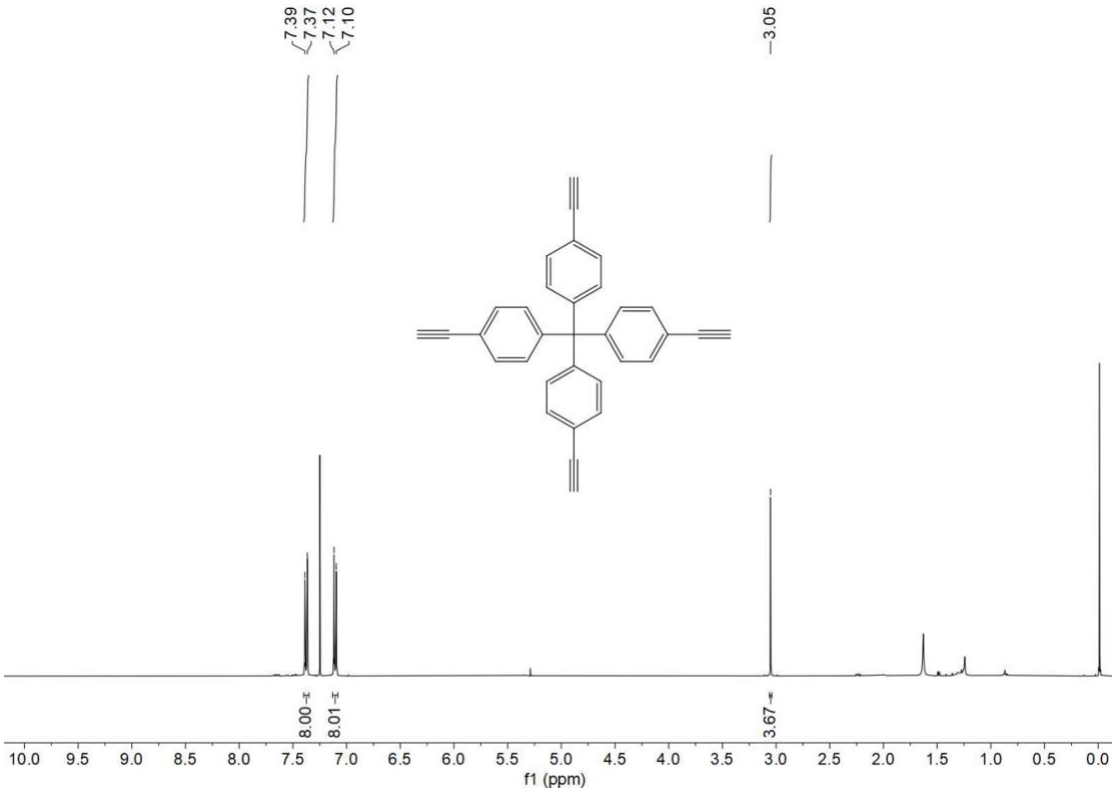

Fig. S9 ^{1}H NMR spectrum of TEPM in $CDCl_3$.

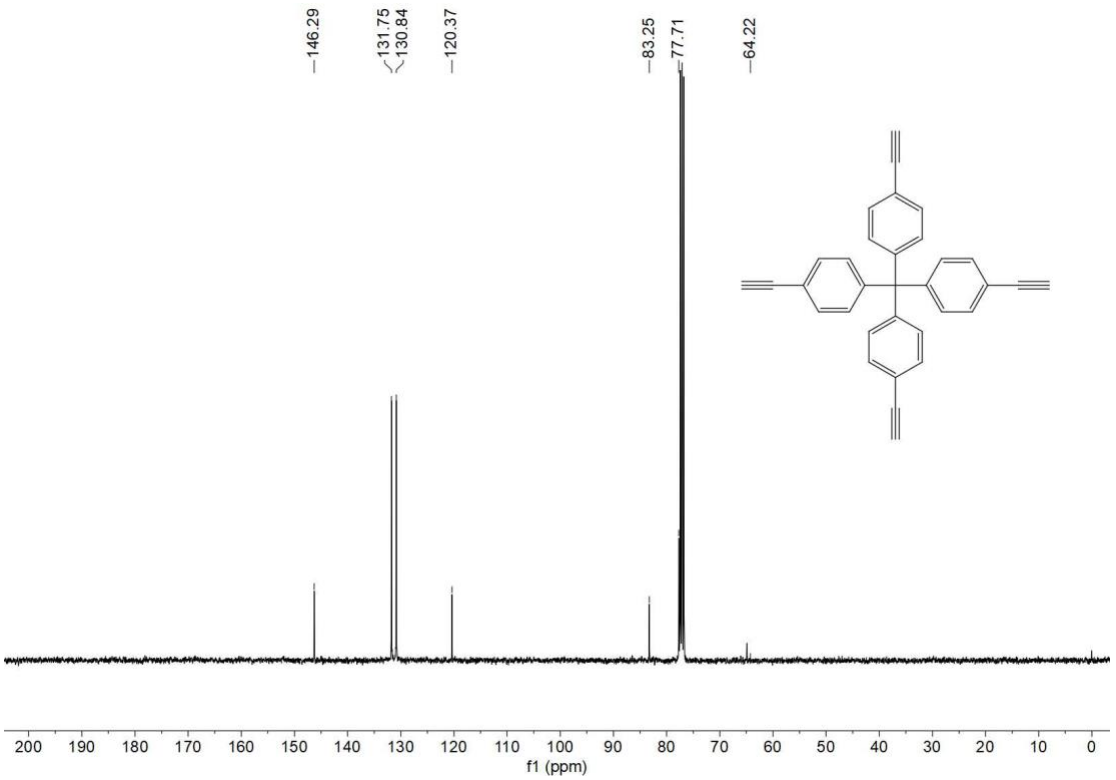

Fig. S10 ^{13}C NMR spectrum of TEPM in $CDCl_3$.

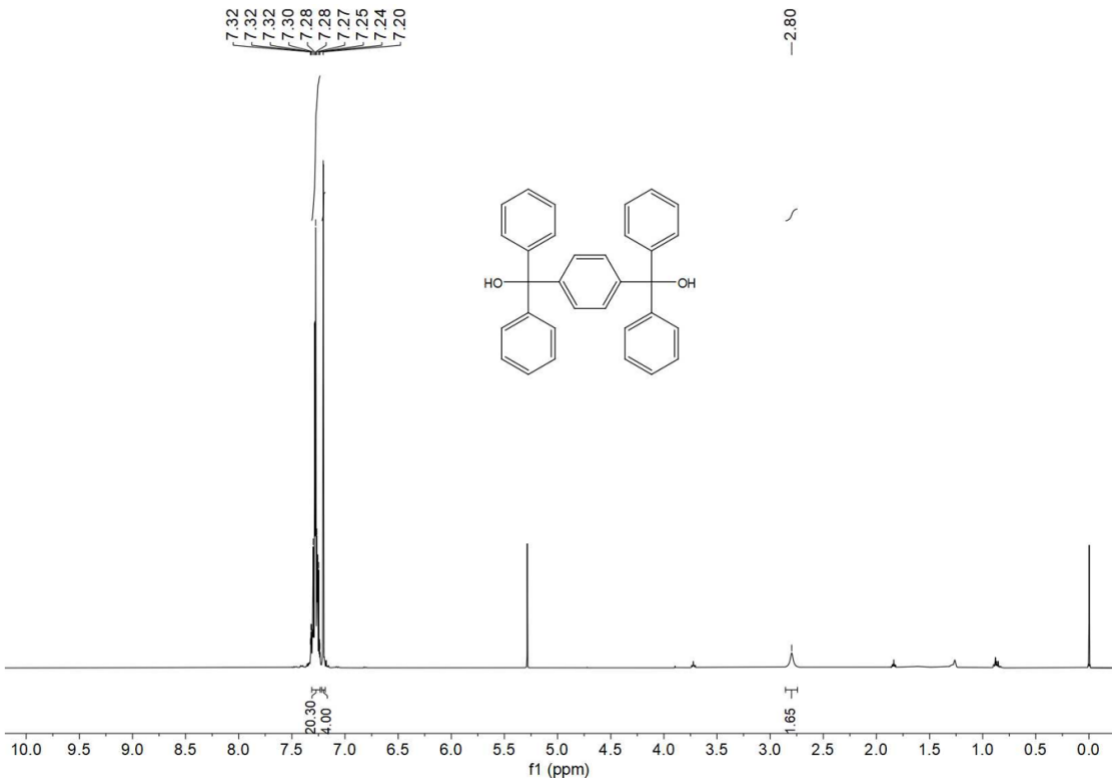

Fig. S11 ^{1}H NMR spectrum of HPM-OH in $CDCl_3$.

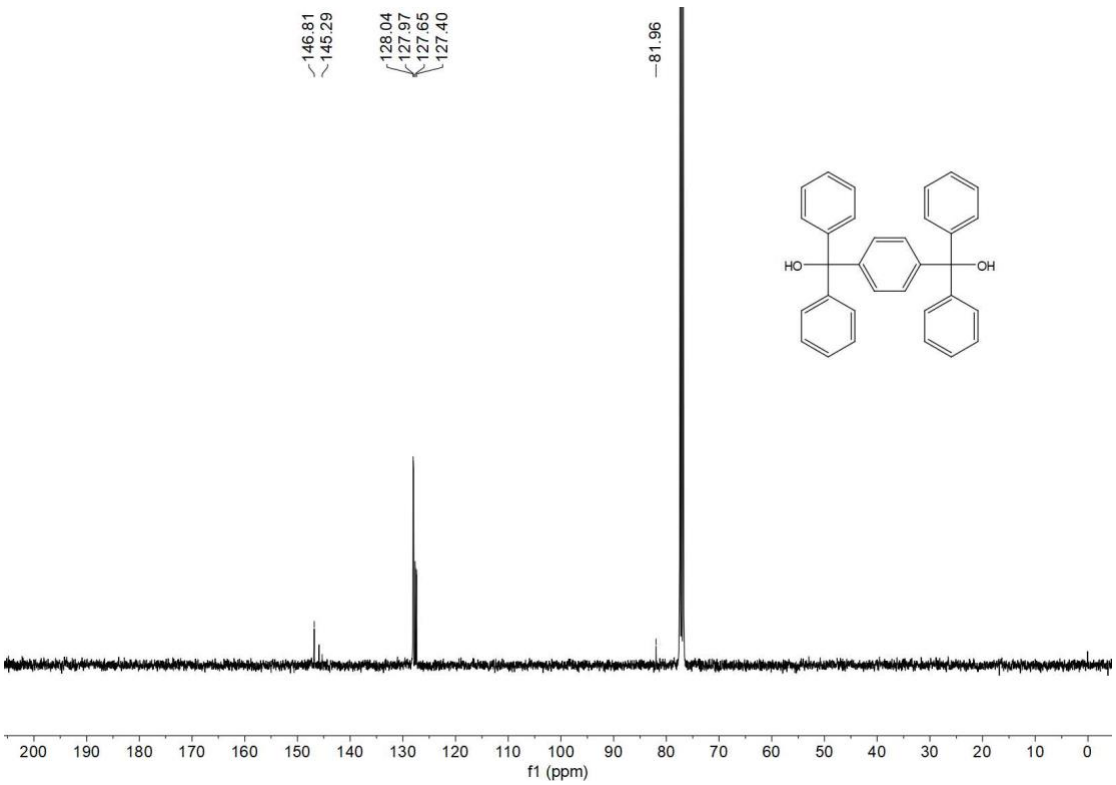

Fig. S12 ^{13}C NMR spectrum of HPM-OH in $CDCl_3$.

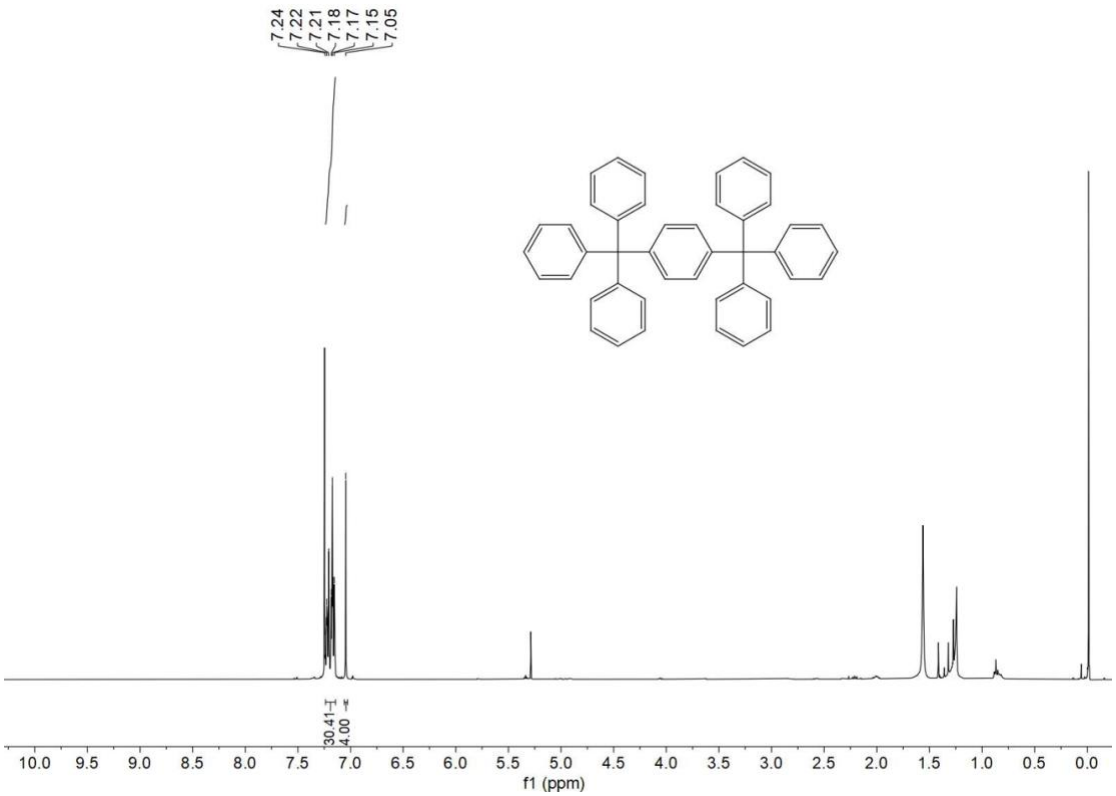

Fig. S13 ^{1}H NMR spectrum of HPM in $CDCl_3$.

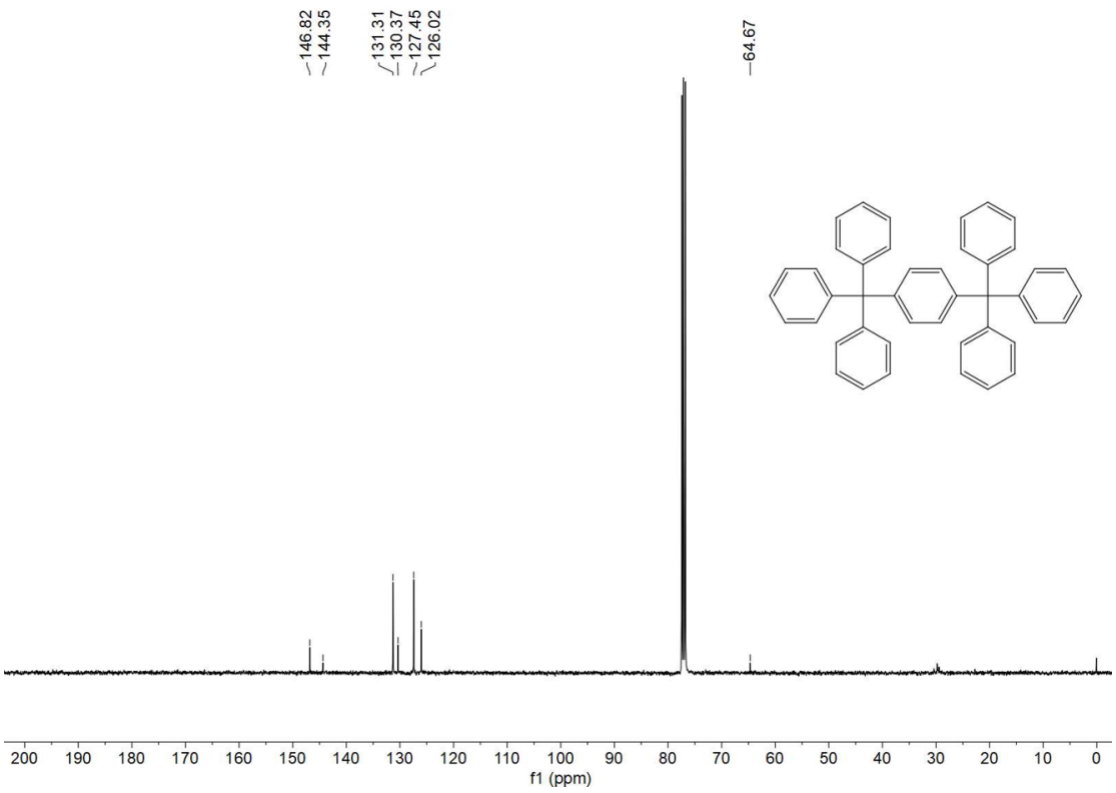

Fig. S14 ^{13}C NMR spectrum of HPM in $CDCl_3$.

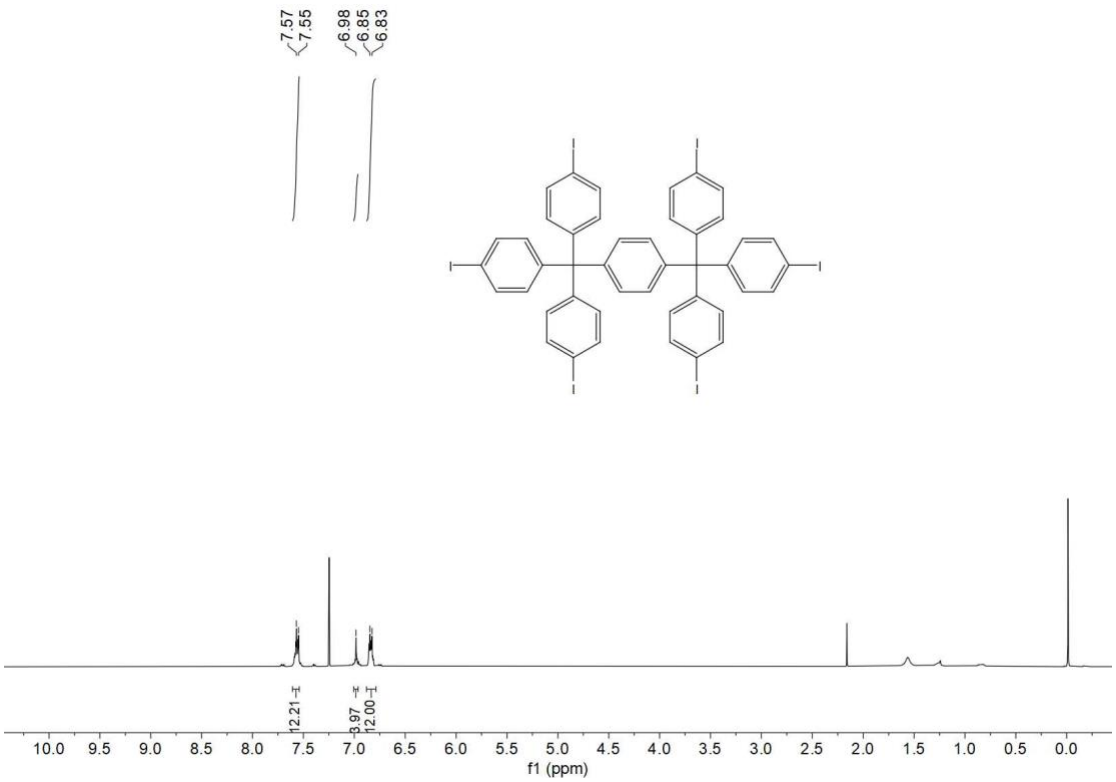

Fig. S15. ^{1}H NMR spectrum of HPM-I in $CDCl_3$.

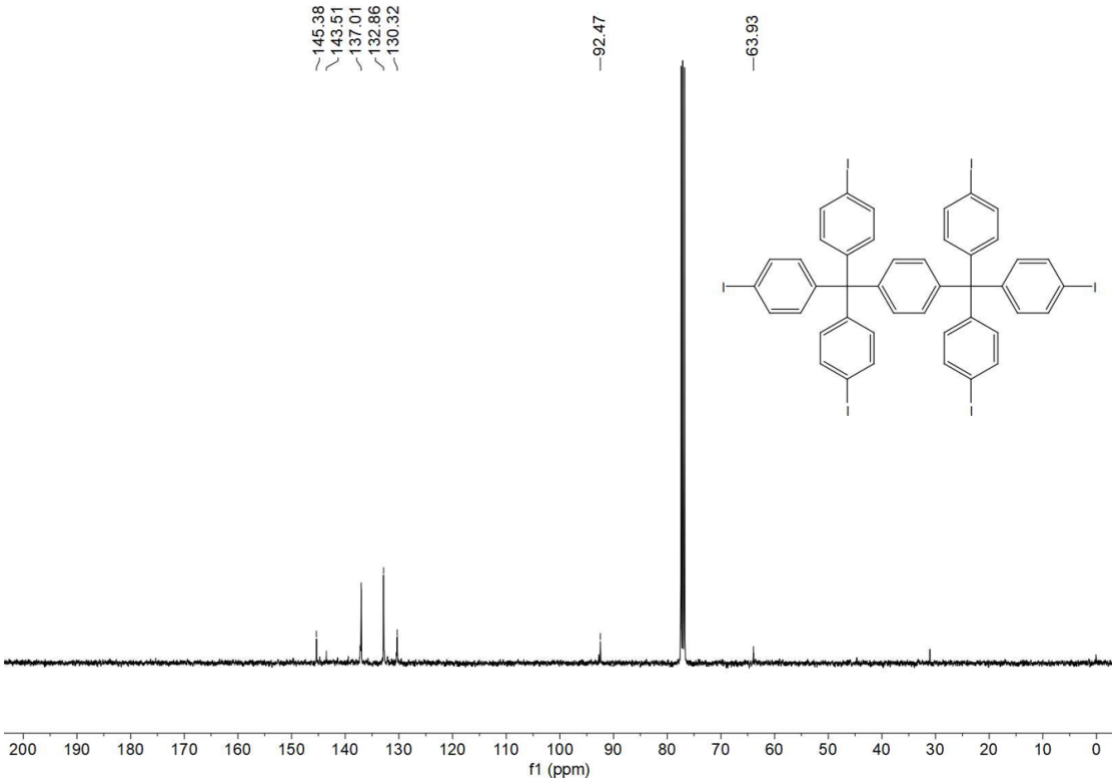

Fig. S16 ^{13}C NMR spectrum of HPM-I in $CDCl_3$.

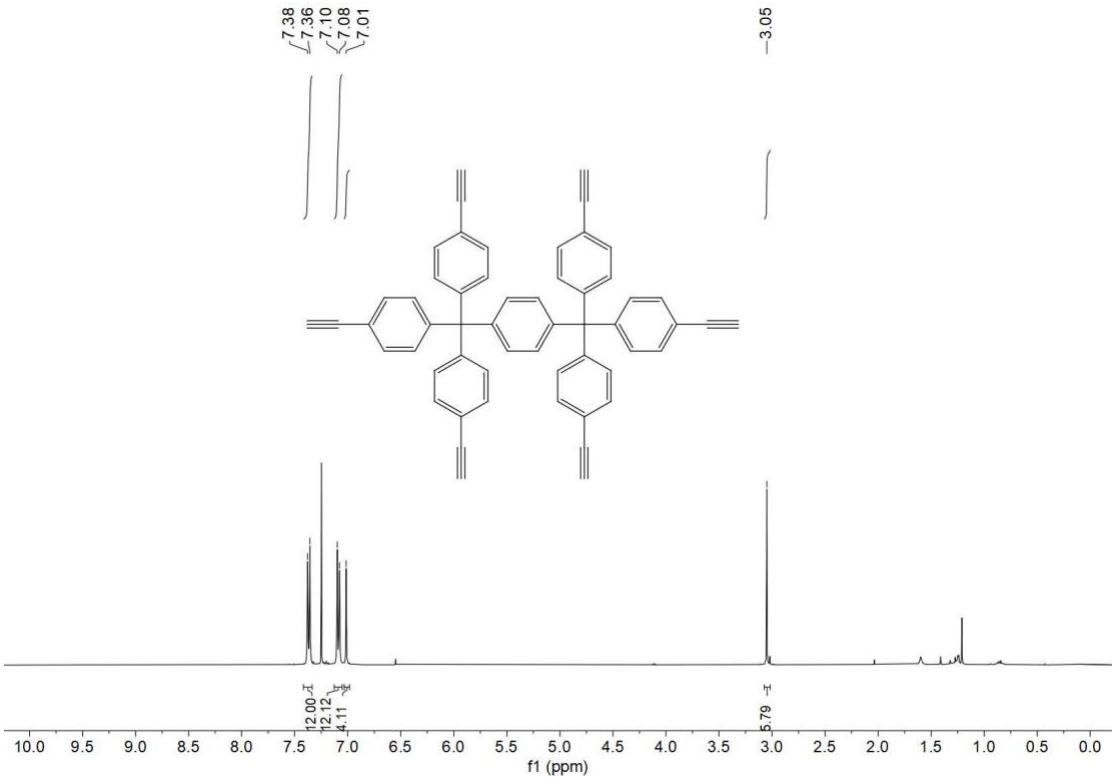

Fig. S17 ^{1}H NMR spectrum of HEPM in $CDCl_3$.

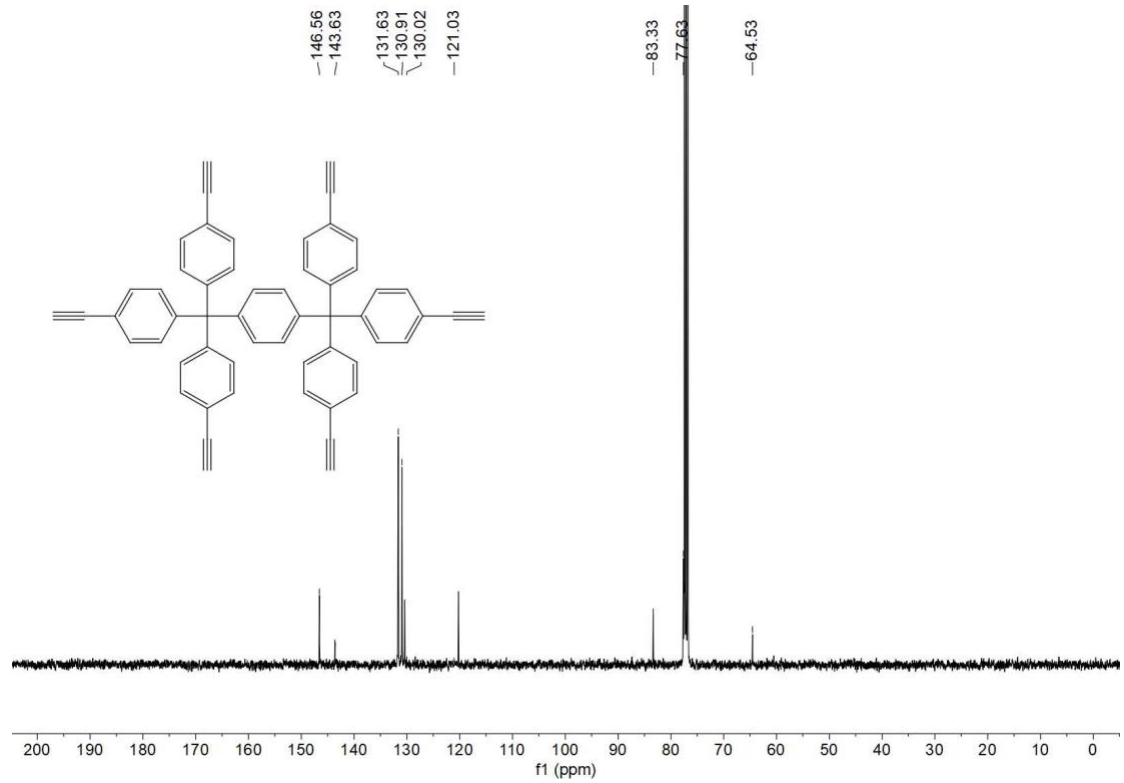

Fig. S18 ^{13}C NMR spectrum of HEPM in $CDCl_3$.

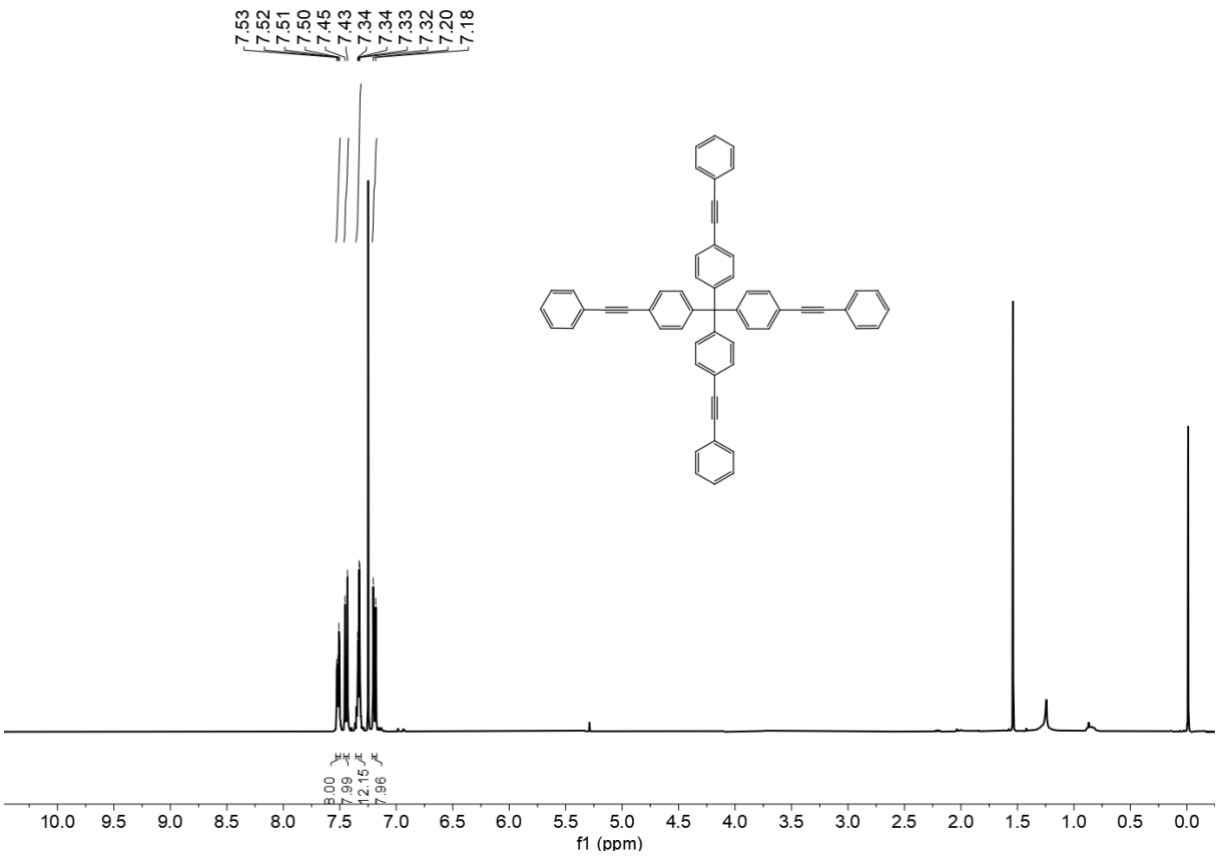

Fig. S19 ^{1}H NMR spectrum of **Ph-TEPM** in $CDCl_3$.

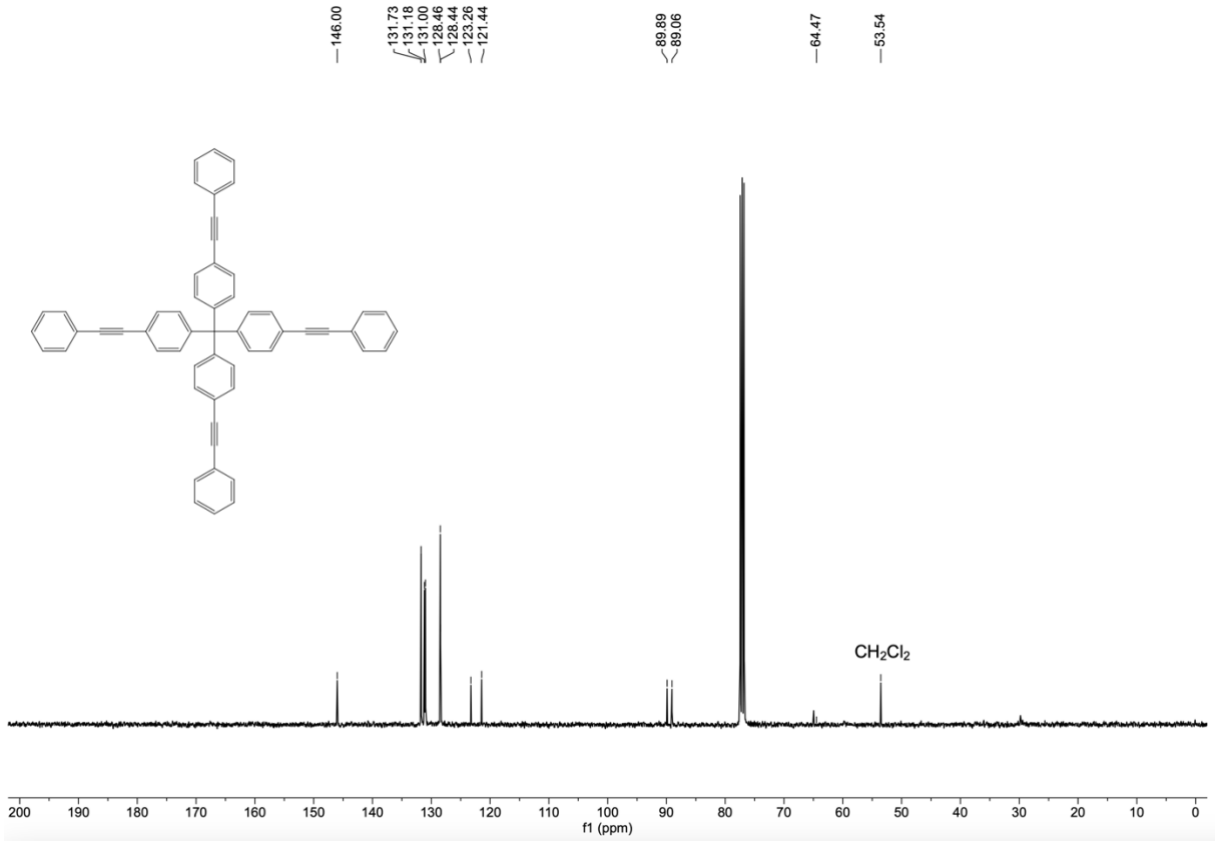

Fig. S20 ^{13}C NMR spectrum of **Ph-TEPM** in $CDCl_3$.

X-ray experimental for *trans*-C[4]P

Diffraction grade single crystals of *trans*-C[4]P were obtained by slow diffusion of ethanol vapor into a dichloromethane solution of the calix[4]pyrrole. A suitable crystal was selected, and the data were collected on a Bruker D8 Venture diffractometer using a μ-focus Cu Kα radiation source (λ = 1.54178 Å) with collimating mirror monochromators. Data were collected using ω-scans. The structures were solved by direct methods using SHELXT[1] and refined by full-matrix least-squares on F2 with anisotropic displacement parameters for the non-H atoms using SHELXL-2018/3. Structure analysis was aided by use of the programs PLATON[3] and OLEX2.

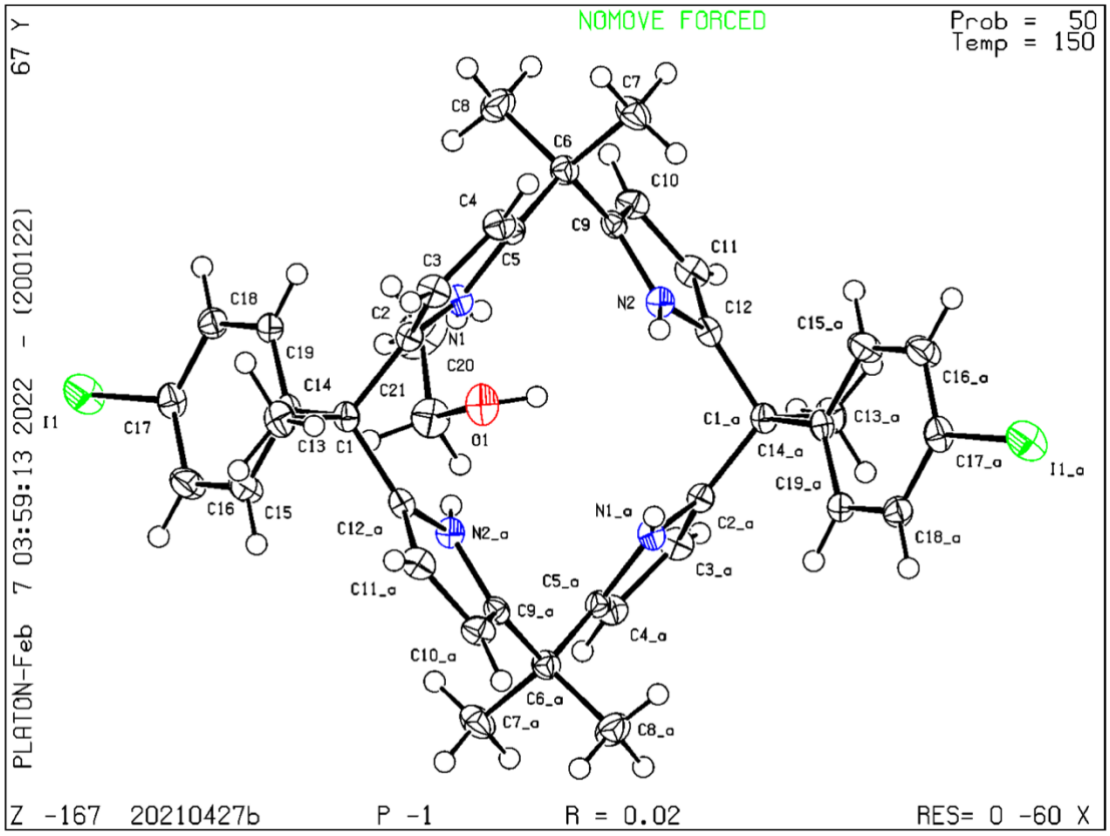

Fig. S21 View of *trans*-C[4]P, which contains one ethanol molecule. N blue, C medium gray, H white, I green.

Table S1 Crystal data and structure refinement for *trans*-C[4]P.

Identification code	20210427b
Empirical formula	$C_{42}H_{50}I_2N_4O_2$
Formula weight	896.66 g/mol
Temperature/K	150(2)
Crystal system	triclinic
Space group	P-1
a/Å	10.0173(6)
b/Å	10.7503(7)
c/Å	10.7734(7)
α/°	100.610(2)
β/°	97.390(2)
γ/°	115.100(2)
Volume/Å^3	1004.42(11)
Z	1
ρ_{calc} g/cm^3	1.482
μ/mm^{-1}	12.595
F(000)	452
Crystal size/mm^3	0.08 × 0.13 × 0.16
Radiation	CuKα (λ = 1.54178 Å)
2Θ range for data collection/°	5.01 to 66.69
Index ranges	$-11 \leq h \leq 11$, $-12 \leq k \leq 12$, $-12 \leq l \leq 12$
Reflections collected	21620
Independent reflections	3494 [R_{int} = 0.0286]
Data/restraints/parameters	3494/0/231
Goodness-of-fit on F^2	1.323
Final R indexes [I>=2σ (I)]	R_1 = 0.0228, wR_2 = 0.0687
Final R indexes [all data]	R_1 = 0.0243, wR_2 = 0.0850
Largest diff. peak/hole / e Å^{-3}	0.906/-0.943
CCDC number	2150418

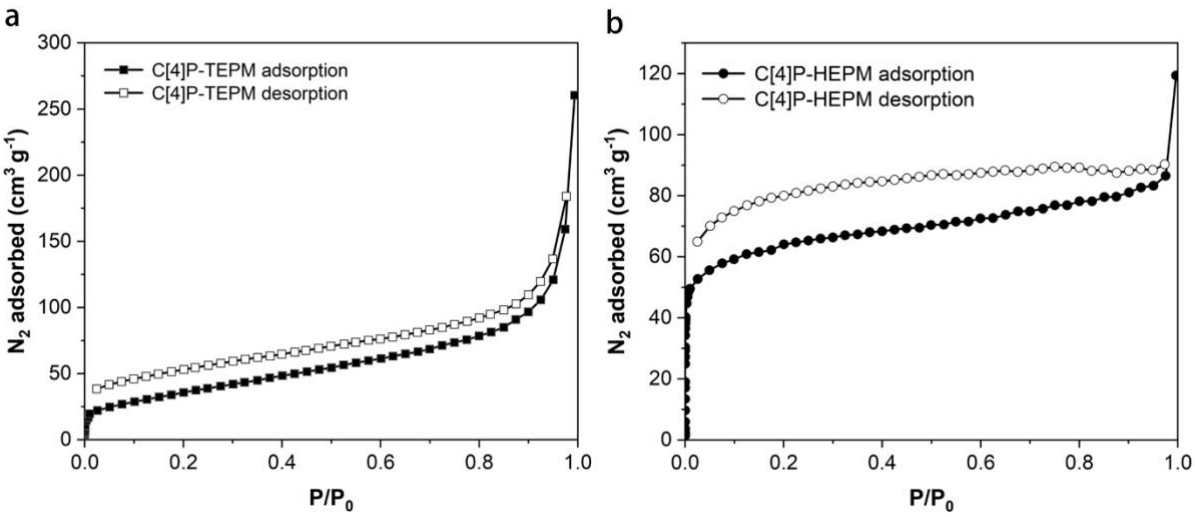

Fig. S22 N_2 sorption isotherms for a) C[4]P-TEPM and b) C[4]P-HEPM at 77 K. Samples were activated by degassed at 100 °C under vacuum for 24 h prior to each N_2 adsorption and desorption analysis.

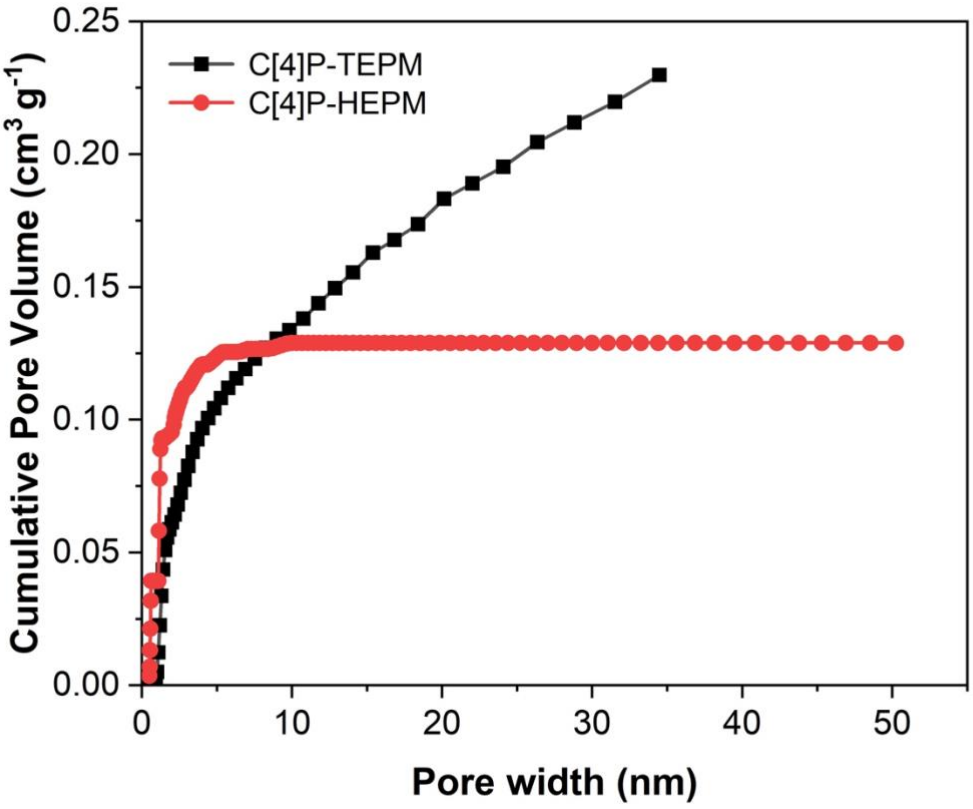

Fig. S23 Cumulative pore volume analysis of C[4]P-TEPM and C[4]P-HEPM obtained using non-local density functional theory (NLDFT).

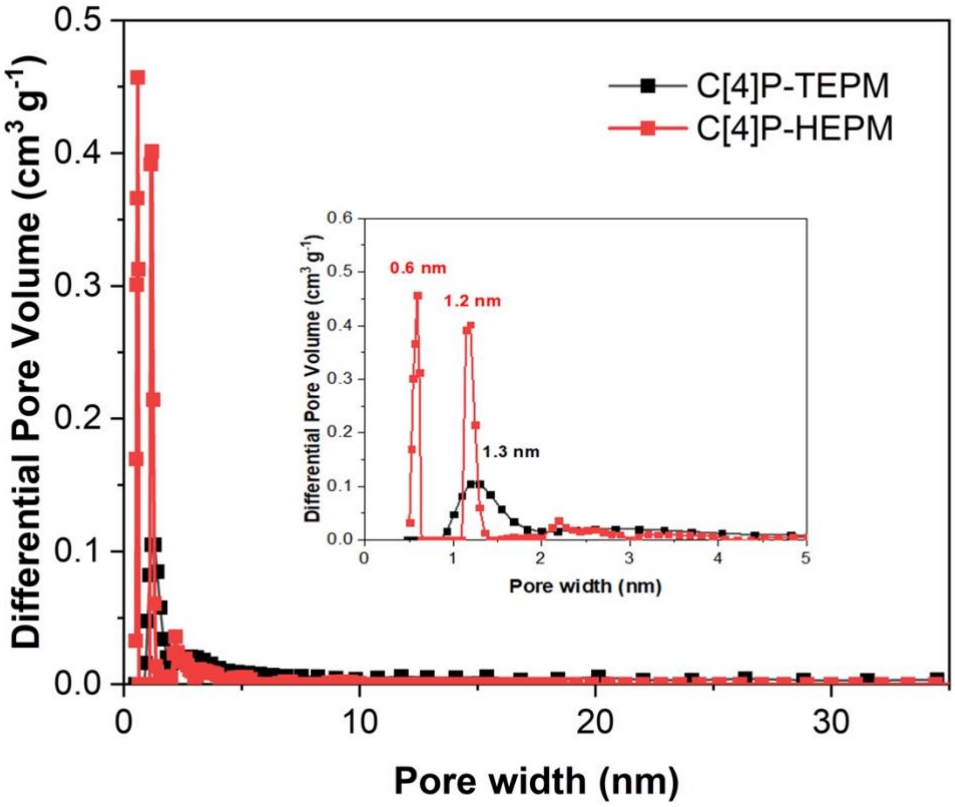

Fig. S24 Pore size distributions of C[4]P-TEPM and C[4]P-HEPM calculated by the NLDFT method.

Table S2 Porosity parameters for the MPNs of the present study.

MPNs	S_{BET} ($m^2\ g^{-1}$)	Pore Volume[a)] ($cm^3\ g^{-1}$)	Pore Width (nm)
C[4]P-TEPM	138.4	0.230	1.299
C[4]P-HEPM	277.6	0.129	0.59 and 1.19

a) Cumulative pore volume calculated by non-local density functional theory from the nitrogen adsorption/desorption experiments shown in Figure S22.

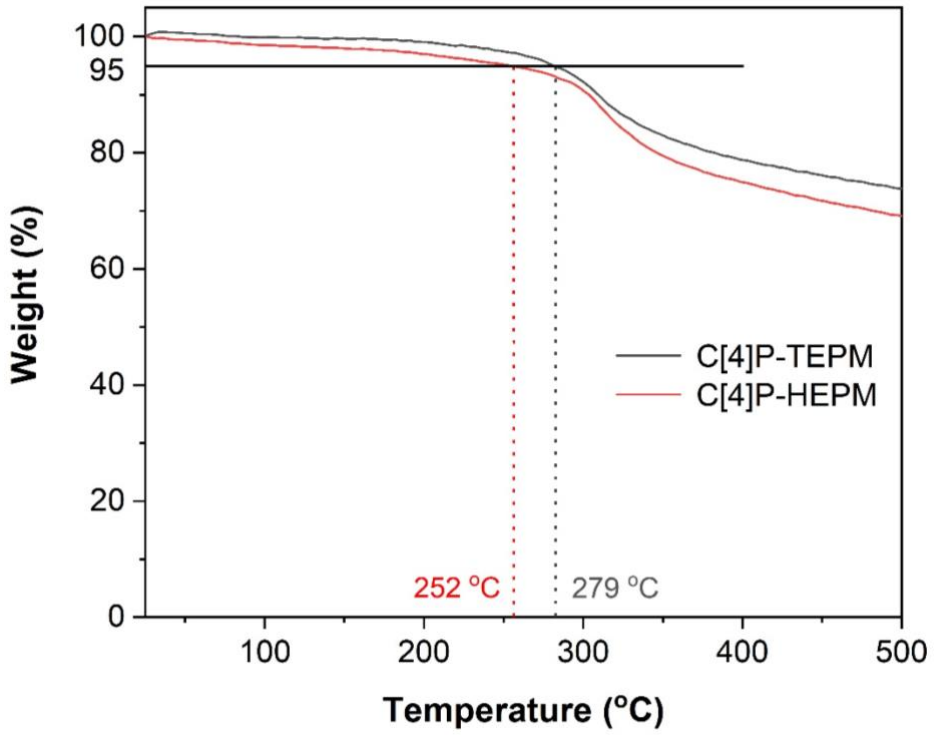

Fig. S25 TGA curves for C[4]P-TEPM and C[4]P-HEPM recorded under an N_2 atmosphere with a heating rate of 10 °C min^{-1}.

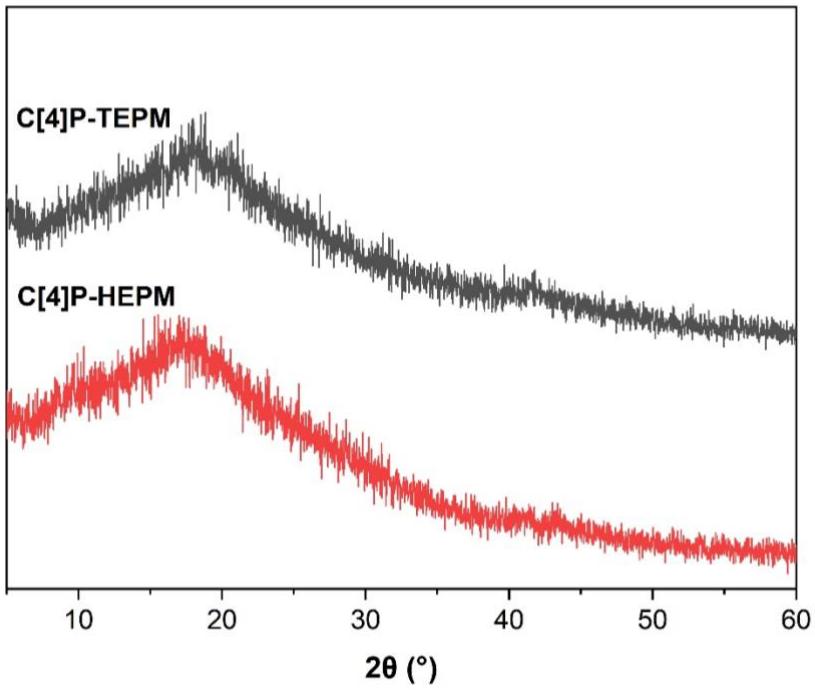

Fig. S26 PXRD patterns for **C[4]P-TEPM** and **C[4]P-HEPM**.

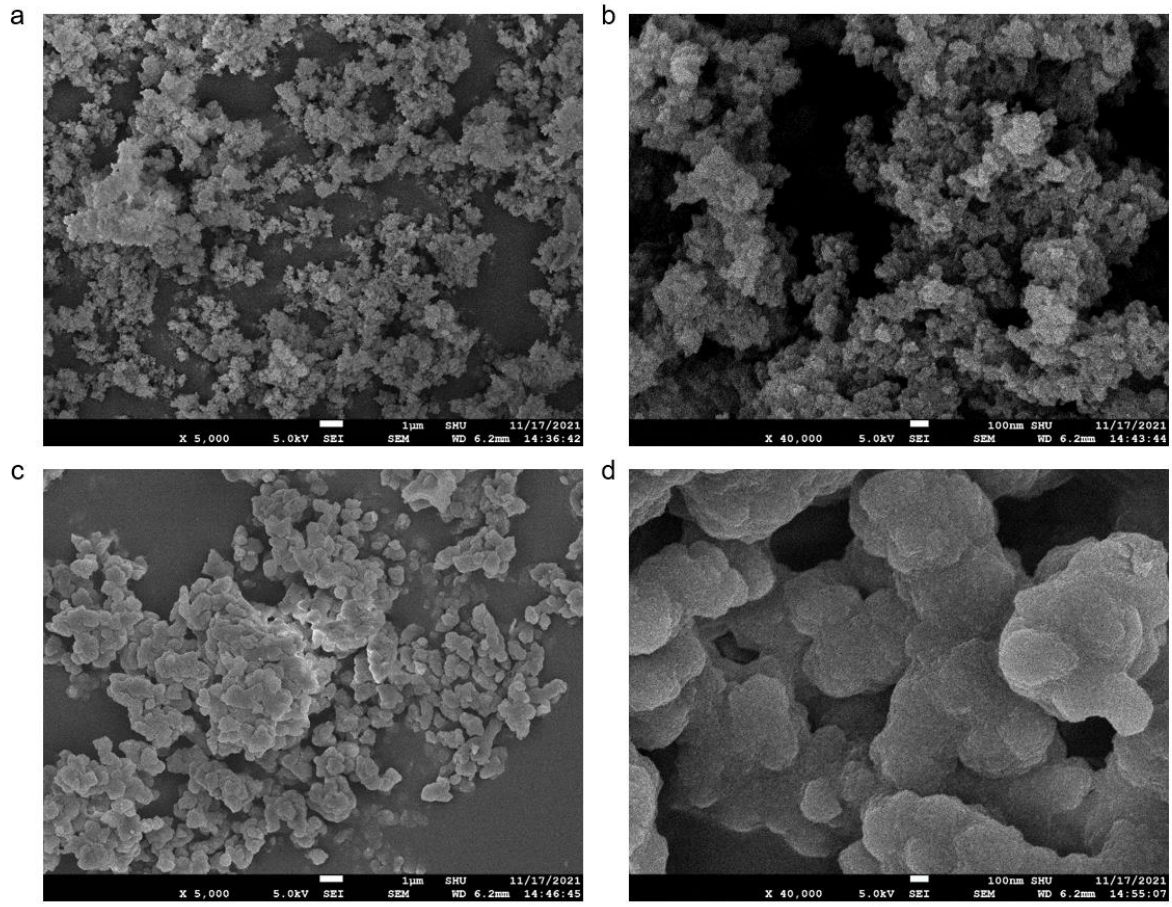

Fig. S27 SEM images of a-b) C[4]P-TEPM and c-d) C[4]P-HEPM with scale bars (white thick line about "SEI" on the x axis) of 1 µm and 100 nm, respectively.

Iodine vapor uptake and release capacity studies

The iodine vapor adsorption capacities of the MPNs of the present study were determined by means of gravimetric analyses. The polymer sample (10 mg) was placed in 5 mL weighing vials, which were pre-weighed before testing and put in 500 mL sealed container with iodine kept at the bottom. The container was kept at 348.15 K at ambient pressure and iodine uptake was determined at different time intervals. After allowing equilibrium to be reached, the vial containing I_2@MPNs was kept at 423.15 K at ambient pressure. Iodine release was then determined by calculating the weight changes in the I_2-loaded materials at different time intervals. The values of uptake capacity are the average values from at least two experiments.

Adsorption from an aqueous iodine source phase

The MPN in question (2.5 mg) was added into a saturated iodine aqueous solution (2.5 mL, 1.2 mM) and stirred at room temperature. After certain time intervals, the concentration of the residual iodine in solution was obtained by filtering off the MPN and recording the UV-Vis spectral intensity of the filtrate. Quantification was effected by comparison to a calibration curve. Removal efficiency was calculated using following equation:

$$\left(\text{Removal efficiency} = \frac{C_0 - C_t}{C_0} \times 100\%\right) \quad (1)$$

where C_0 (mM) and C_t (mM) are the concentrations within the aqueous solution before and after treating with the MPN.

The amount of iodine adsorbed from the aqueous source phase was determined using the following equation:

$$\left(q_t = \frac{(C_0 - C_t)\ M_w}{m \times 1000}\right) \quad (2)$$

where q_t (g g^{-1}) is the amount of iodine adsorbed per g of adsorbent at time t (min). C_0 (mM) and C_t (mM) are the same as above and are the initial and residual concentrations of the aqueous source and post MPN treatment filtrate, respectively. Mw (g mol^{-1}) is the molecular mass of iodine; m (g g^{-1}) is the mass of the polymer used in the study.

Selective adsorption experiments

The MPN under study (3 mg) was added to an aqueous iodine solution (3 mL, 1.2 mM) containing 12 mM of KF, KCl, KBr, and K_2SO_4, respectively. The solution was then stirred

for 20 min. The concentrations of the iodine in solution after filtering were determined via UV-Vis spectral analysis. The removal efficiency was calculated using equation (1).

Adsorption kinetics

Pseudo-first-order (equation 3) and pseudo-second-order (equation 4) models were used to fit the adsorption kinetics.

$$(\ln(q_e - q_t) = \ln q_e - k_1 t) \quad (3)$$

Where q_e and q_t represent the amount of iodine adsorption (mg g^{-1}) at equilibrium and the amount of iodine adsorbed (mg g^{-1}) at any given time, t, respectively. k_1 (min^{-1}) is the pseudo-first-order rate constant corresponding to the adsorption kinetics per this model.

$$(\frac{t}{q_t} = \frac{t}{q_e} + \frac{1}{k_{obs}\, q_e^2}) \quad (4)$$

where q_t is amount of iodine adsorbed from aqueous solution (g g^{-1}) at time t (min); qe is the adsorbate uptake (g g^{-1}) at equilibrium. k_{obs} is a second-order rate constant (g g^{-1} min^{-1}), which can be calculated from the intercept and slope of a plot of t/qt against t.

Iodine adsorption capacity in saturated I_2 aqueous solution

The MPN (10 mg) sample was added into the round bottom flask containing 200 mL of saturated iodine aqueous solutions (1.2 mM) and stirred at room temperature for 24 h. The iodine-loaded MPN was filtered off, and the UV-Vis spectral intensity of the filtrate was recorded. Quantification was determined by comparison to a calibration curve. The uptake capacity was calculated using equation (2). The recorded iodine uptake capacity is the average of two independent experiments.

Iodine adsorption capacity from aqueous KI/I_2 solutions

Gravimetric analyses. MPN samples (10 mg, 30 mg or 50 mg) were placed in a round bottom flask containing 3.0 g KI, 1.5 g I_2 and 6 mL water. The mixture was stirred at room temperature for 36 h. The samples were collected by filtration, washed with water, and dried in the air to afford a black solid. The filtrate was collected and subjected to a bisulfite starch titration as detailed below.

Bisulfite starch titration. 5 mL of a 1% aqueous starch indicator solution was added into the combined filtrate and washings and the resulting solution slowly titrated with an aqueous 0.05

M sodium bisulfite solution until the original blue colour was discharged. The iodine adsorption capacity of the MPN in question was then calculated from the net change in the iodine content in the starting and post-MPN exposure aqueous solutions.

Recyclability performance studies

The polymer sample (12.5 mg) was added into an aqueous iodine solution (280 mL, 1.2 mM) and stirred at room temperature for 48 h. After filtering, the concentration of the iodine in solution was measured using a UV-Vis spectrophotometer. I_2@MPN was immersed into ethanol and ultrasonicated for 2 h to promote iodine release. After filtering and drying in vacuum at 40 °C for 24 h, the regenerated sample was used for the next adsorption cycle. This process was repeated 4 times.

Reaction between Ph-TEPM and iodine.

Electrophilic additions between iodine and alkynes are not expected on the basis of energetics. In order to rule out this putative concern on the basis of experiment, we synthesized a model compound, **Ph-TEPM**, which contains the tetrakis(4-ethynylphenyl)methane building block. We then exposed this alkyne both to a saturated iodine aqueous solution and iodine vapor at 150 °C. In the first of these tests, **Ph-TEPM** (10 mg) was added into a round bottom flask containing 20 mL of saturated aqueous iodine (1.2 mM) and stirred at room temperature for 24 h. The resulting material (denoted **Ph-TEPM-a**) was filtered off, and charactered directly by ^{1}H NMR spectroscopy without further purification. In the second study, **Ph-TEPM** (10 mg) was placed in a weighing vial (5 mL), which was put in a 100 mL sealed container with iodine (800 mg) at the bottom. After being held at 423.15 K at ambient pressure for 24 h, the resulting material (termed **Ph-TEPM-b**) was collected and measure directly by ^{1}H NMR spectroscopy. The ^{1}H NMR spectra of **Ph-TEPM-a** and **Ph-TEPM-b** (Fig. S28) confirmed the expectation that there was no change in the alkyne moiety.

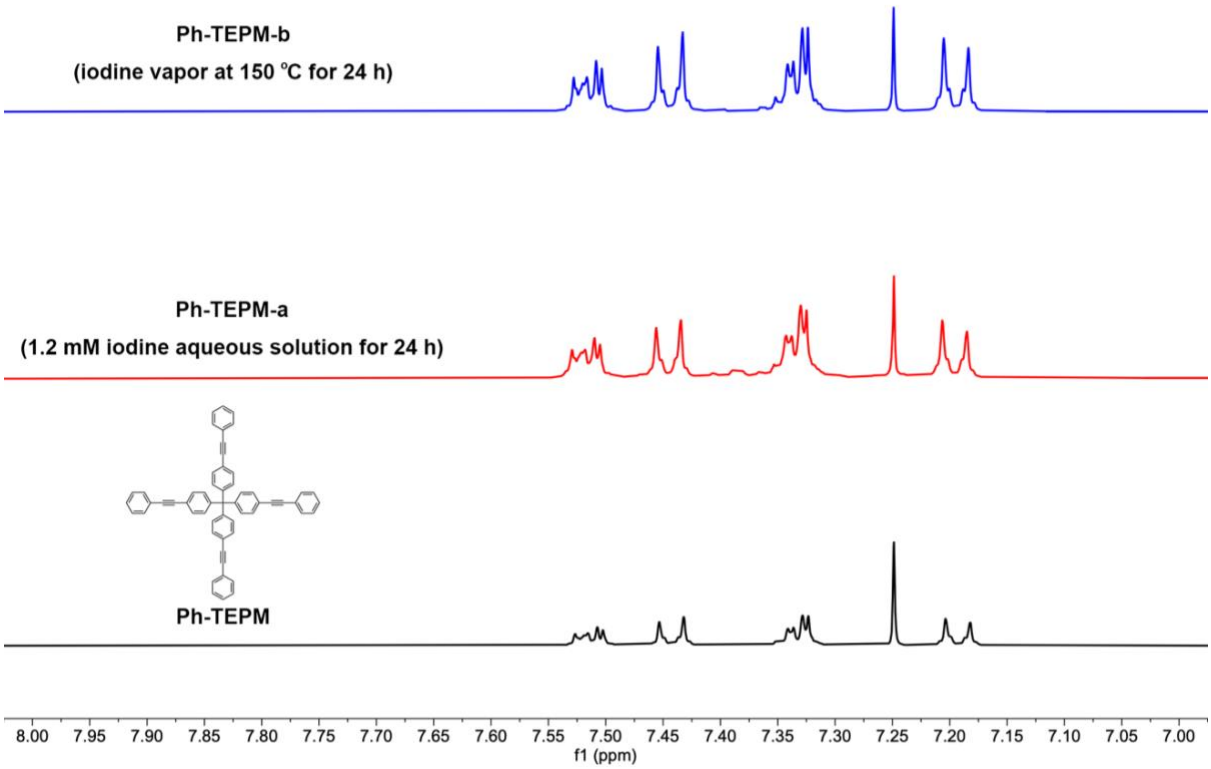

Fig. S28 ^{1}H NMR spectra of the model compound **Ph-TEPM** and daughter materials termed **Ph-TEPM-a** and **Ph-TEPM-b**.

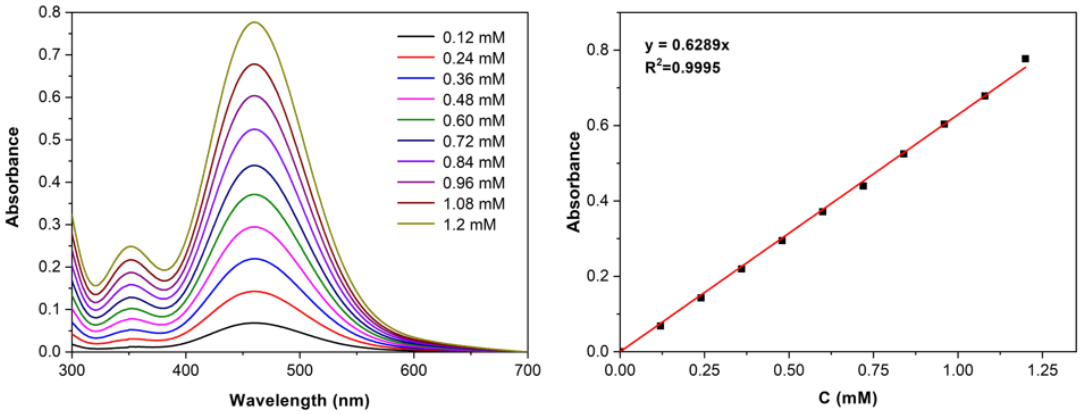

Fig. S29 UV-Vis spectra of aqueous iodine solutions of different concentrations (left). Standard curve plotted based on the absorbance at 460 nm (right).

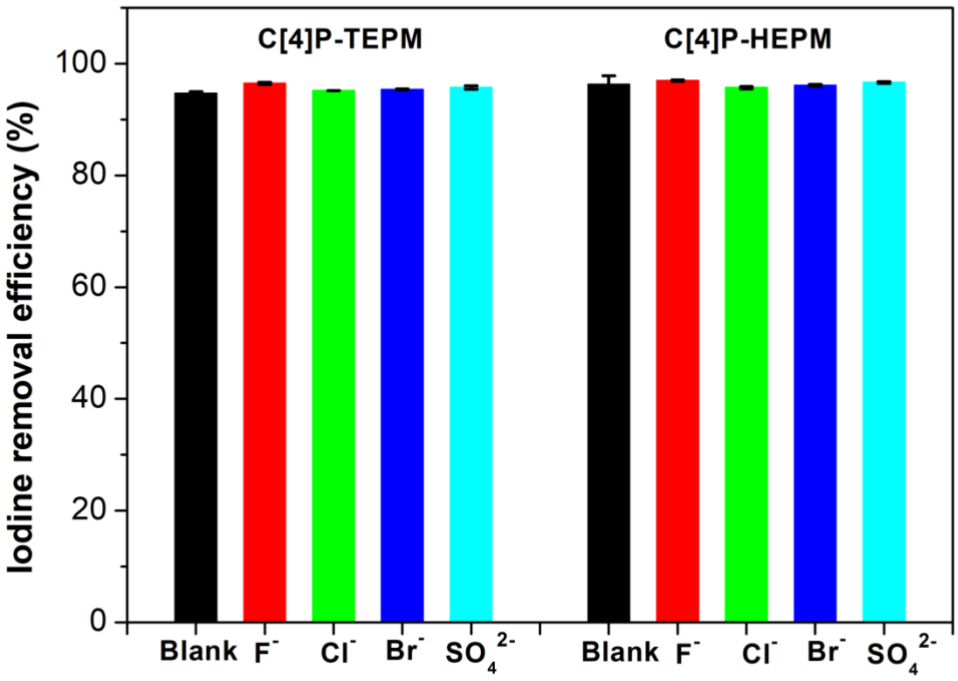

Fig. S30 Removal efficiencies of C[4]P-TEPM and C[4]P-HEPM for saturated iodine aqueous solutions (1.2 mM) in the presence of competing anions (as their potassium salts).

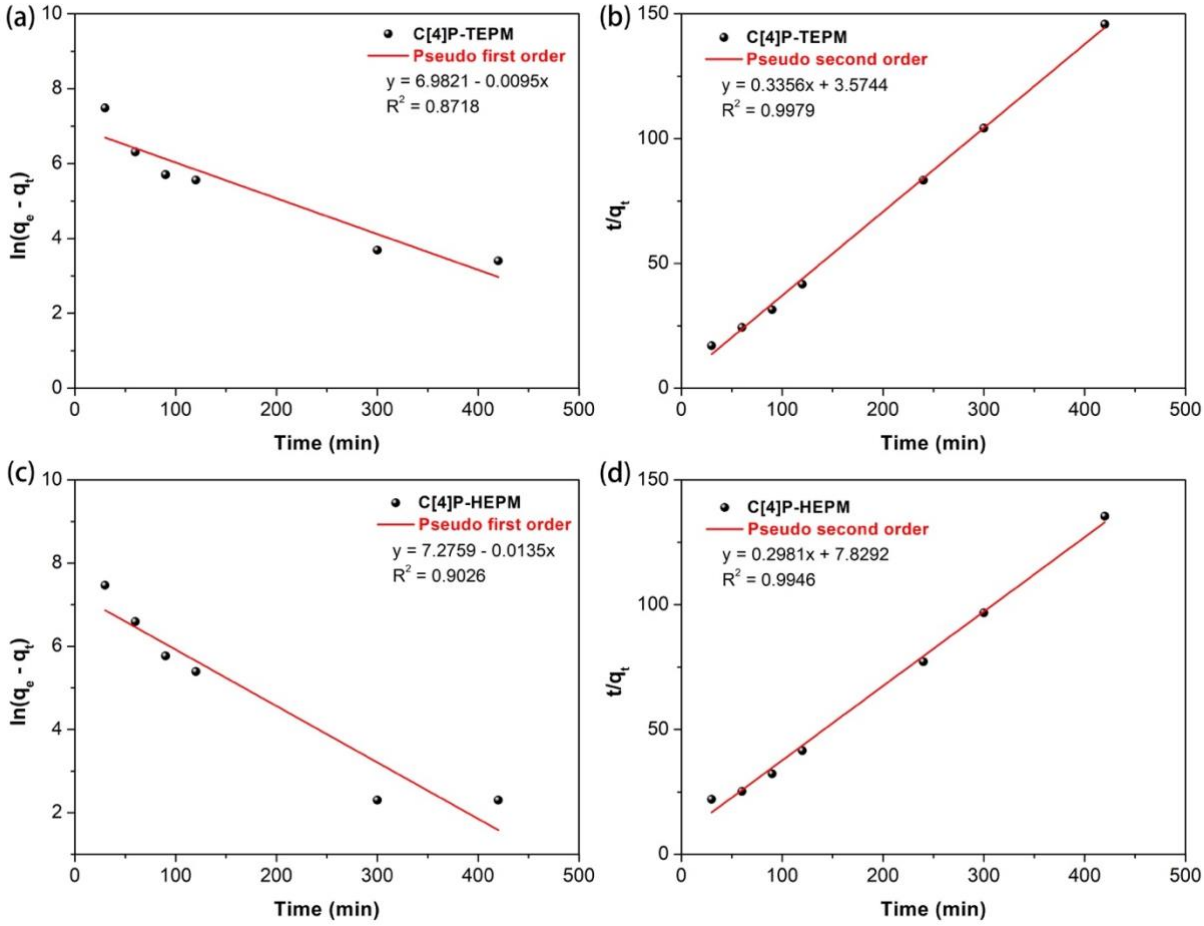

Fig. S31 Pseudo-first-order and pseudo-second-order adsorption kinetic plots of iodine vapor uptake by C[4]P-TEPM (a and b) and C[4]P-HEPM (c and d), respectively.

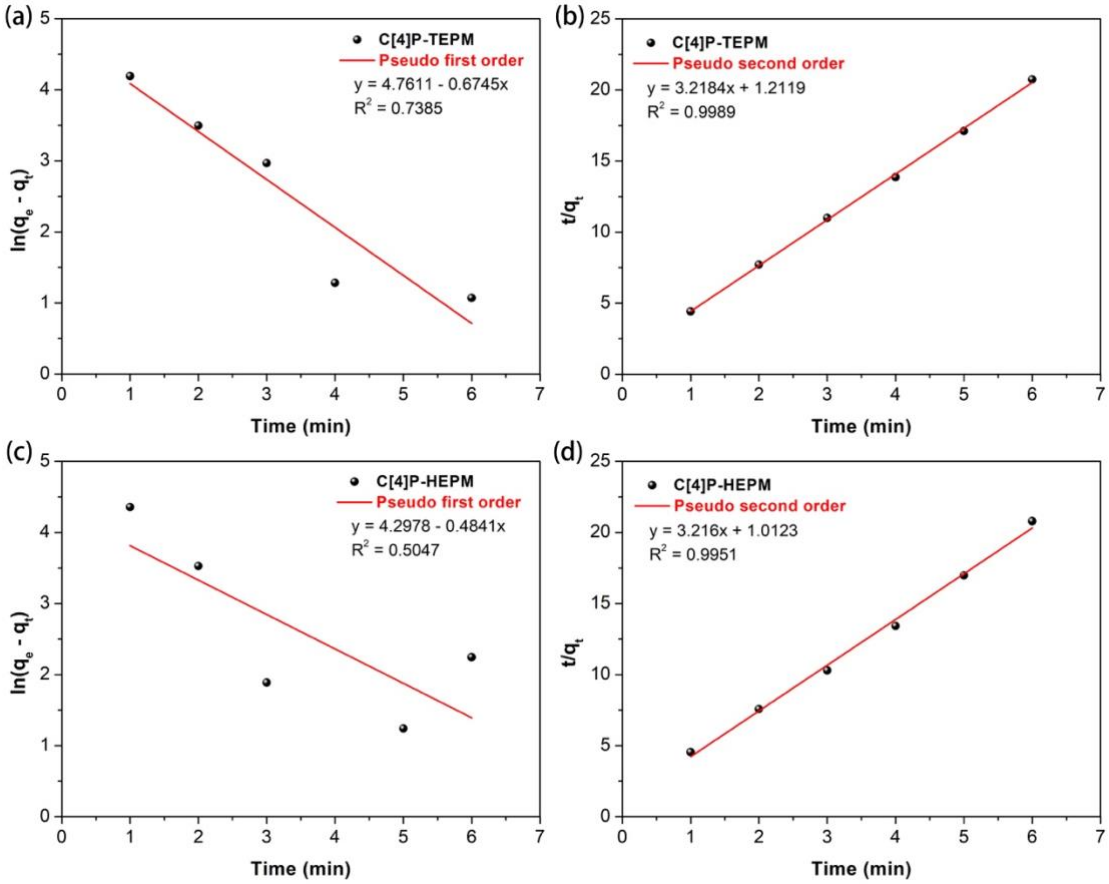

Fig. S32 Pseudo-first-order and pseudo-second-order adsorption kinetic plots corresponding to the uptake of iodine from saturated aqueous solutions (1.2 mM in all cases) by C[4]P-TEPM (a and b) and C[4]P-HEPM (c and d), respectively.

Table S3 Iodine uptake capacities from aqueous KI/I_2 solutions.

MPNs	Mass (mg)	I_2 uptake capacity from gravimetric analyses ($g\ g^{-1}$)	I_2 uptake capacity from bisulfite starch titration ($g\ g^{-1}$)
C[4]P-TEPM	10	4.18	4.06
	30	4.05	4.03
	50	4.16	3.96
C[4]P-HEPM	10	5.01	4.45
	30	4.52	4.49
	50	4.60	4.42

Table S4. Iodine uptake capacities and adsorption rates of different adsorbent materials from aqueous source phases.

Materials	Iodine uptake capacity ($g\ g^{-1}$)	k_{obs} ($g\ g^{-1}\ min^{-1}$)	Type	Reference
C[4]P-HEPM	4.45	10.2169	POP	This work
C[4]P-TEPM	4.02	8.5469	POP	This work
N-MOF-PAN fibers	3.56	1.43	MOF	*ACS Appl Mater Interfaces*, 2022, **14**, 47126-47136.
C[4]P-BTP	3.24	7.814	POP	*Angew Chem Int Ed*, 2022, **61**, e202113724.
C[4]P-TPE	2.99	3.286	POP	*Angew Chem Int Ed*, 2022, **61**, e202113724.
PTIBBL	0.6667	0.807	POP	*Chem Commun*, 2020, **56**, 1401-1404.
calixpyridinium–PyTS	0.455	0.01517	calixpyridinium	*Langmuir*, 2021, **37**, 11422-11428.

Table S5 Iodine adsorption capacities of different adsorbent materials for capture experiments involving saturated aqueous iodine solutions.

Number	Materials	Iodine uptake capacity (g g^{-1})	Concentration of iodine aqueous solution	Type	Reference
41	**C[4]P-HEPM**	4.45	KI/I_2 aqueous solution	MPN	This work
40	**C[4]P-TEPM**	4.02	KI/I_2 aqueous solution	MPN	This work
39	**C[4]P-HEPM**	4.07	Saturated I_2 aqueous solution	MPN	This work
38	**C[4]P-TEPM**	3.67	Saturated I_2 aqueous solution	MPN	This work
37	**HcOF-4**	3.57	KI/I_2 aqueous solution	COF	*J Am Chem Soc*, 2019, **141**, 10915-10923.
36	**N-MOF-PAN fibers**	3.56	KI/I_2 aqueous solution	MOF	*ACS Appl Mater Interfaces*, 2022, **14**, 47126-47136.
35	**Compound 1**	3.55	KI/I_2 aqueous solution	POP	*ACS Appl Mater Interfaces*, 2021, **13**, 34188-34196.
34	**C[4]P-BTP**	3.24	KI/I_2 aqueous solution	MPN	*Angew Chem Int Ed*, 2022, **61**, e202113724.
33	**HcOF-2**	3.23	KI/I_2 aqueous solution	COF	*J Am Chem Soc*, 2019, **141**, 10915-10923.
32	**C-poly- 1_5**	3.2258	the Langmuir isotherm model	POP	*Chem Sci*, 2022, **13**, 1111-1118.
31	**CaCOP3**	3.1	KI/I_2 aqueous solution	Calix[4]arenes (POP)	*Mater Chem Phys*, 2020, **239**, 122328-122333.
30	**Compound 2**	3.04	KI/I_2 aqueous solution	POP	*ACS Appl Mater Interfaces*, 2021, **13**, 34188-34196.
29	**HcOF-3**	3.00	KI/I_2 aqueous solution	COF	*J Am Chem Soc*, 2019, **141**, 10915-10923.
28	**C[4]P-TPE**	2.99	KI/I_2 aqueous solution	MPN	*Angew Chem Int Ed*, 2022, **61**, e202113724.
27	**CaCOP2**	2.81	KI/I_2 aqueous solution	Calix[4]arenes (POP)	*Mater Chem Phys*, 2020, **239**, 122328-122333.
26	**PIL**	2.57	50 mL of 200 ppm aqueous solution of iodine	PIL	*New J Chem*, 2019, **43**, 1117-1121.
25	**C[4]P-TTP**	2.51	KI/I_2 aqueous solution	MPN	*Angew Chem Int Ed*, 2022, **61**, e202113724.
24	**CaCOP1**	2.4	KI/I_2 aqueous solution	Calix[4]arenes (POP)	*Mater Chem Phys*, 2020, **239**, 122328-122333.
23	**C[4]P-BP**	2.37	KI/I_2 aqueous solution	MPN	*Angew Chem Int Ed*, 2022, **61**, e202113724.
22	**C[4]P-BT**	2.32	KI/I_2 aqueous solution	MPN	*Angew Chem Int Ed*, 2022, **61**, e202113724.
21	**CalCOP1**	2.32	KI/I_2 aqueous solution	Polycalix[4]arenes	*J Mater Sci*, 2020, **55**, 1854-1864.
20	**COF@NH_2-MOF**	2.157	the Langmuir isotherm model	Composite materials	*Environ Sci Pollut Res*, 2022, **29**, 88882-88893.
19	**HcOF-1**	2.1±0.1	KI/I_2 aqueous solution	COF	*J Am Chem Soc*, 2017, **139**, 7172-7175.
18	**CalCOP2**	1.758	KI/I_2 aqueous solution	Polycalix[4]arenes	*J Mater Sci*, 2020, **55**, 1854-1864.
17	**PCN-223**	1.677	the Langmuir isotherm model	MOF	*Sep Purif Technol*, 2020, **233**, 115999-116005.
16	**PCN-223-HPP**	1.616	the Langmuir isotherm model	MOF	*Sep Purif Technol*, 2020, **233**, 115999-116005.
15	**C[4]P-DPP**	1.58	KI/I_2 aqueous solution	MPN	*Angew Chem Int Ed*, 2022, **61**, e202113724.
14	**3D MOF-1**	1.1±0.05	KI/I_2 aqueous solution	MOF	*ACS Appl Mater Interfaces*, 2020, **12**, 46107-46118.

13	**TAPB-BPDA**	0.988	the Langmuir isotherm model	COF	*React Funct Polym*, 2021, **159**, 104806-104813.
12	**NH_2-MOF**	0.94	the Langmuir isotherm model	MOF	*Environ Sci Pollut Res*, 2022, **29**, 88882-88893.
11	**THPS-C**	0.926	the Langmuir isotherm model	Triptycene	*Adv Mater Interfaces*, 2019, **6**, 1900249-1900254.
10	**AlMC-1**	0.89	KI/I_2 aqueous solution	aluminum macrocycle-faced cages	*Nat Commun*, 2022, **13**, 6632-6641.
9	**Zn(ttr)(OAc)**	0.8461	the Langmuir isotherm model	MOF	*Environ Sci Pollut Res*, 2021, **28**, 28797-28807.
8	**Fe_3O_4/COF**	0.797	5 mL of 0.2 g/L aqueous solution of iodine	COF	*ACS Macro Lett*, 2017, **6**, 1444-1450.
7	**Zn(tr)(OAc)**	0.7145	the Langmuir isotherm model	MOF	*Environ Sci Pollut Res*, 2021, **28**, 28797-28807.
6	**PTIBBL**	0.6667	the Langmuir isotherm model	POP	*Chem Commun*, 2020, **56**, 1401-1404.
5	**calixpyridinium–PyTS**	0.455	760 mg/L aqueous solution of iodine	Calixpyridinium	*Langmuir*, 2021, **37**, 11422-11428.
4	**MIL-125-NH_2@chitosan**	0.399	the Langmuir isotherm model	MOF	*Carbohydr Polym*, 2020, **231**, 115742-11552.
3	**CalCOP3**	0.346	KI/I_2 aqueous solution	Polycalix[4]arenes	*J Mater Sci*, 2020, **55**, 1854-1864.
2	**SCNU-Z4**	0.332	KI/I_2 aqueous solution	MOF	*Inorg Chem Front*, 2021, **8**, 1083-1092.
1	**CalCOP4**	0.156	KI/I_2 aqueous solution	Polycalix[4]arenes	*J Mater Sci*, 2020, **55**, 1854-1864.

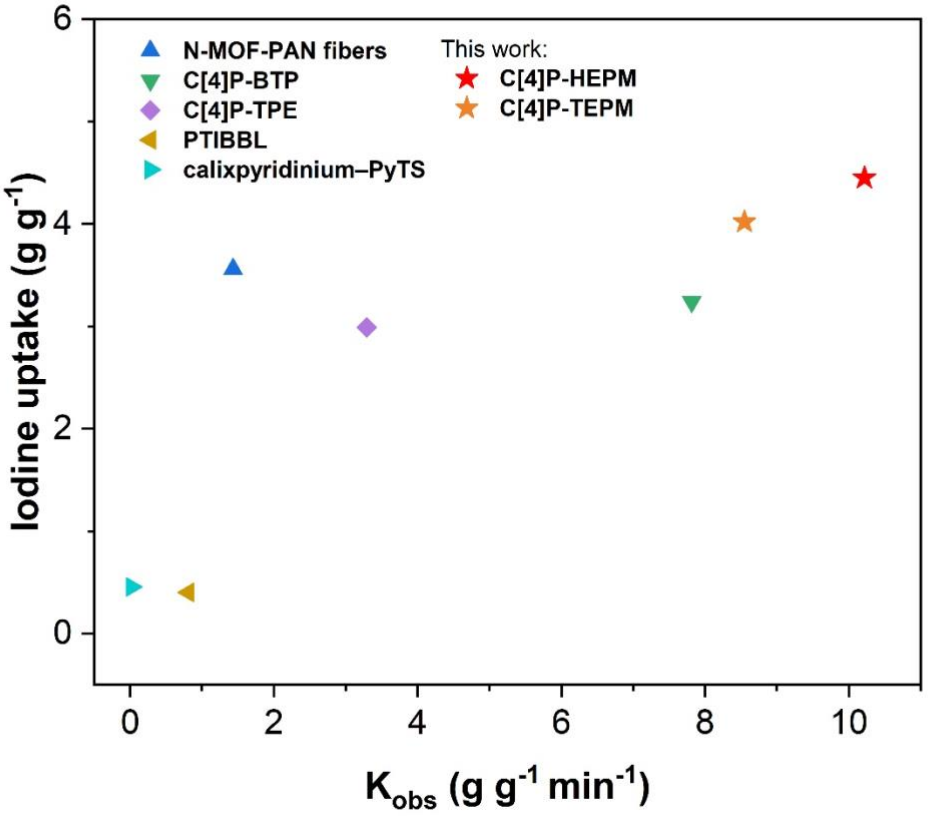

Fig. S33 Comparisons of iodine adsorption capacities and rates of uptake for different adsorbents in capture experiments involving an aqueous source phase. The orange and red stars represent C[4]P-TEPM and C[4]P-HEPM as detailed in the present report. The corresponding adsorption data and references are provided in Table S4.

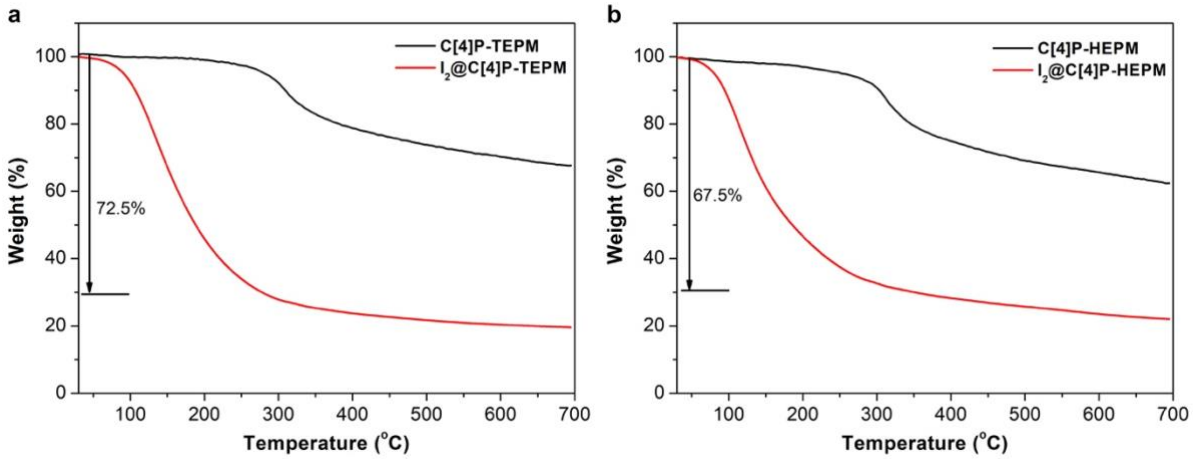

Fig. S34 TGA curves of C[4]P-TEPM and I_2@C[4]P-TEPM (a), and C[4]P-HEPM and I_2@C[4]P-HEPM (b) under an N_2 atmosphere at a heating rate of 10 °C min^{-1}.

Supplementary References

[1] V. Valderrey, E. C. Escudero-Adan and P. Ballester, *J Am Chem Soc*, 2012, **134**, 10733-10736.

[2] W. Lu, D. Yuan, D. Zhao, C. Schilling, O. Plietzsch, T. Muller, S. Bräse, J. Guenther, J. Blümel, R. Krishna, Z. Li and H. Zhou, *Chem Mater*, 2010, **22**, 5964-5972.

[3] J.-I. Urzúa and M. Torneiro, *J Org Chem*, 2017, **82**, 13231-13238.

[4] O. Plietzsch, A. Schade, A. Hafner, J. Huuskonen, K. Rissanen, M. Nieger, T. Muller and S. Bräse, *European Journal of Organic Chemistry*, 2013, **2**, 283-299.